Controlling radical intermediates in photocatalytic conversion of low-carbon-number alcohols

Zhuyan Gao [†,‡], Nengchao Luo [†,*], Zhipeng Huang [†,‡], Stuart H. Taylor [§], and Feng Wang [†,*]

[†] State Key Laboratory of Catalysis, Dalian National Laboratory for Clean Energy, Dalian Institute of Chemical Physics, Chinese Academy of Sciences, Dalian, 116023, China.

[‡] University of Chinese Academy of Sciences, Beijing, 100049, China.

[§] Cardiff Catalysis Institute, School of Chemistry, Cardiff University, Main Building, Park Place, Cardiff, CF10 3AT, UK.

* Corresponding Author.

*N. L.: e-mail, ncluo@dicp.ac.cn.

*F. W.: e-mail, wangfeng@dicp.ac.cn.

ABSTRACT

Low-carbon number alcohols (LCNAs) are important platform molecules that can be derived from many resources, such as coal, oil, natural gas, biomass, and CO_2, creating a route to value-added chemicals and fuels. Semiconductor photocatalysis provides a novel method for converting LCNAs into a variety of downstream products. Photocatalysis is initiated by light-excited charge carriers that are highly oxidative and reductive. The polarity and bond dissociation energy (BDE) of C_α−H bonds are small for alcohols, so it can be homolytically dissociated by the participation of photogenerated holes. Consequently, photocatalytic LCNA conversion overcomes the challenge of C_α−H bond activation in thermocatalysis. Apart from carbon radicals generated from C_α−H bond cleavage, many other radicals are formed during photocatalysis, which are active and have multiple conversion pathways, resulting in complex product distributions. In this perspective, we summarize the methods of controlling the generation of radical intermediates and subsequent reactions in photocatalytic conversion of LCNAs. The intrinsic properties of photocatalysts and external solution environments are the two main factors that affect the selectivity of the final products. On this basis, we summarize the challenges in current photocatalytic conversion of LCNAs and propose directions for future research, with the aim to inspire studies on the selective conversion of small molecular radicals.

Keywords: alcohols; photocatalysis; radical; selectivity control; C_α−H bond

INTRODUCTION

Low-carbon number alcohols (LCNAs, $C_nH_{2n+1}OH$, $n < 4$), including methanol, ethanol, 1-propanol, and isopropanol, are produced from a wide range of raw feedstocks, such as fossil resources,[1-4] biomass,[5-6] and CO_2,[7] by pathways such as oxidation, hydrogenation, hydration, and fermentation. LCNAs can be converted to various downstream products *via* thermocatalytic processes. For instance, they can be oxidized to their corresponding carbonyl compounds[8] and organic acids,[9] or be converted to nitriles or amines,[10-12] ethers,[13] esters,[14] and longer-chain chemicals[15-16] *via* ammoxidation, dehydration, esterification, and the Guerbet reaction. Recently, with the development of the hydrogen energy economy, LCNAs are used as promising hydrogen carriers due to their high hydrogen content (12.5 wt%, 13.0 wt%, and 13.3 wt% for methanol, ethanol, and 1-propanol or isopropanol, respectively), and their convenience for storage and transportation.[17] Catalytic reforming of aqueous alcohol solutions allows for the production of H_2 in high yields.[18-19] H_2 is a promising clean energy carrier which has a high heating value and is free from emission of polluting combustion product.[20-21] As a result, the wide range of resources for LCNAs production together with the facile conversion processes makes LCNAs important platform molecules, which creates a route from natural carbon resources to many value-added chemicals.

The hydrogen atoms in LCNAs are connected *via* three types of covalent bonds: The O−H bond of the hydroxyl group (−OH), the C_α−H bond adjacent to the −OH, and other C−H bonds distanced from the −OH. Generally, the O−H bond and the C_α−H bond are more likely to be

activated, but the ways in which the chemical bonds are cleaved are different. The O−H bond is highly polar, and the electrons constituting this bond are biased towards the oxygen atom, and the bond dissociation energy (BDE) of the O−H bond is high (> 430 kJ mol^{-1}).[22] Thus, the O−H bond is inclined to dissociate heterolytically. On the contrary, the C_α−H bond is less polar and the BDE is relatively low (< 400 kJ mol^{-1}),[22] and could tend to favor homolytic dissociation to a larger extent. While the heterolysis of the C_α−H bond is more complicated than that of the O−H bond. Thermocatalytic conversion of alcohols usually follows the mechanism of heterolytic dissociation of chemical bonds.[23] Reactions requiring the activation of C_α−H bond, *e.g.*, dehydrogenation, are usually carried out either at high temperature[8, 24] (> 573 K) or in the presence of oxidants.[25] The challenges associated with the heterolysis of C_α−H bond in LCNAs can be circumvented by activating it homolytically. However, C_α−H bond homolysis remains a huge challenge for the current thermocatalytic method due to the presence of more reactive −OH in LCNAs. Therefore, effective ways to preferentially activate the C_α−H bond need to be developed.

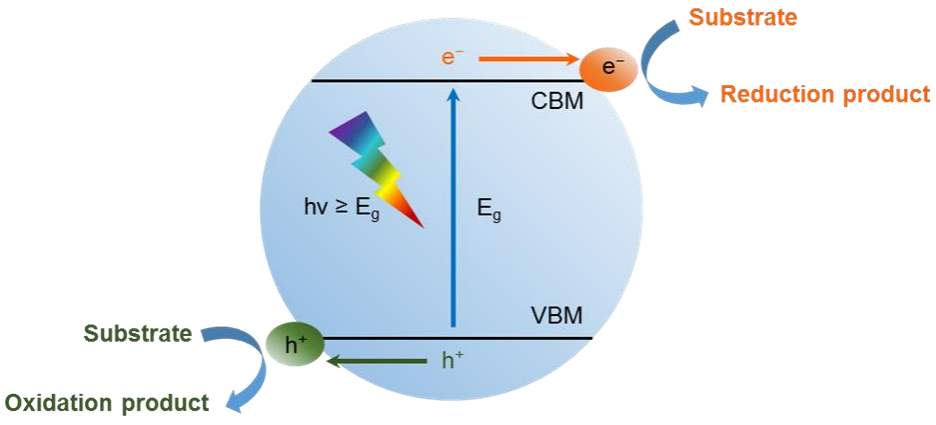

Figure 1. Schematic illustration of elementary steps of photocatalysis over semiconductors. CBM: conduction band minimum; VBM: valence band maximum; E_g: band gap energy. Adapted with

permission from ref 29. Copyright 2019 Royal Society of Chemistry.

Solar energy is the most abundant energy source on the earth. The average solar energy reaching the surface of the earth is estimated to be 5.89×10^{20} J h^{-1}, which is almost 1.2 times the global energy consumption per year. The utilization of solar energy is an imperative topic of sustainable development.[26-27] Processes that directly convert solar energy into chemical energy, such as water splitting and CO_2 reduction,[28-31] have been pursuit in recent decades. The mechanism of photocatalysis involves three steps (Figure 1). Initially, photocatalysts are irradiated by photons with energy larger than the bandgap energy of the semiconductor, generating oxidative holes and reductive electrons. Photogenerated holes and electrons then separate and migrate from the bulk of the photocatalyst to the surface. Finally, holes and electrons induce oxidation and reduction reactions, respectively. Homolytic cleavage of C_α−H bond in photocatalytic LCNAs conversion is realized by the participation of photogenerated holes while the O−H bond with larger BDE is harder to oxidize by photogenerated holes and it is more readily preserved in the final products, which is beneficial to obtain oxygenated products. Due to utilizing the solar energy to drive chemical reactions, the hydrogen from C−H or O−H bond cleavage will be evolved as H_2. Hence, photocatalytic alcohol splitting readily affords H_2 as well as products from dehydrogenation or C−C bond coupling when the photocatalyst is irradiated by light.[32-35]

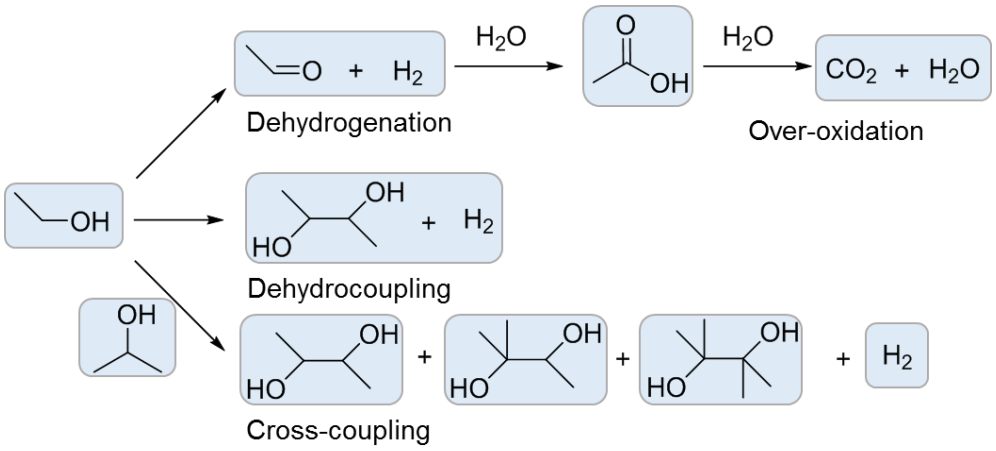

Figure 2. Overview of the conversion processes and products of photocatalytic conversion of ethanol.

Controlling the product selectivity in the photocatalytic conversion of LCNAs is still often overlooked, and it is challenging. Photocatalytic conversion of LCNAs usually proceed *via* radical mechanisms and involve many active species, like hydroxyl radicals (•OH), 1-hydroxyalkyl radicals and alkoxyl radicals. These radicals undergo dehydrogenation, oxidation, and coupling reactions to generate complex products involving carbonyl compounds, organic acids, vicinal diols, and over-oxidized products with the participation of water or oxidants (Figure 2). In this perspective, we summarize methods, including tuning the size, surface polarity, geometry, and surface defects of semiconductors to control radical intermediates involved in photocatalytic LCNA conversion. Suitable reduction cocatalysts and using appropriate reaction solutions to tune the products are also discussed. These approaches aim to tune the generation and subsequent reactions of radical intermediates. Finally, challenges of photocatalytic LCNA conversion emerging from current studies are highlighted, such as establishing direct characterization methods for short-lived molecular radicals and developing efficient methods to control radical intermediates.

Radical Intermediates Generation and Their Subsequent Reactions during Photocatalytic LCNA Conversion

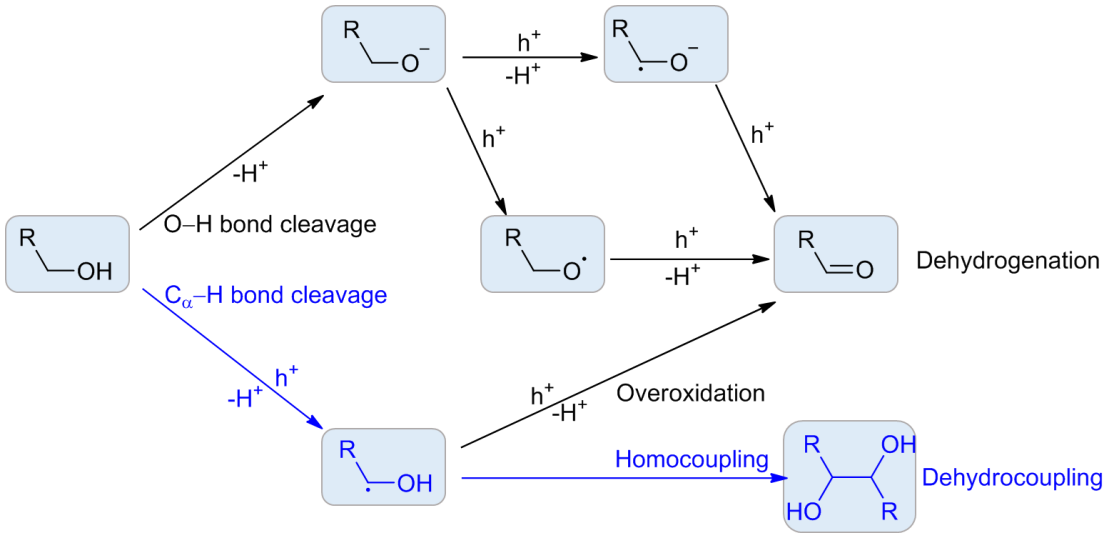

Figure 3. Proposed reaction network of photocatalytic dehydrogenation and dehydrocoupling of LCNAs.

Photocatalytic conversion of LCNAs include oxidation with the participation of oxidants, dehydrogenation and dehydrocoupling in oxidant-free conditions, and transfer hydrogenation using LCNAs as hydrogen donors. Due to the presence of oxidants, the final products are carbonyl compounds or over-oxidation products.[36-37] Photocatalytic dehydrogenation and dehydrocoupling of LCNAs are competing reactions and are conducted in an inert atmosphere. The selectivity of the final products is influenced by radical intermediates produced from the oxidation or reduction of LCNAs and their subsequent reaction pathways. The proposed reaction network is shown in Figure 3. When the activation of LCNAs begins with O−H bond heterolysis, the final products are carbonyl compounds. On the contrary, when homolytic cleavage of C_{α}−H bond occurs first, the

final products depend on the subsequent reaction of the 1-hydroxyalkyl radical intermediates. These radical intermediates can be further oxidized to carbonyl compounds by photogenerated holes, or diffuse into the bulk solvent and couple with each other to produce vicinal diols. Consequently, either the initial activation of LCNA bonds or the subsequent reactions determines the final products. The two pathways mentioned above can be affected by a number of factors, including physical and chemical structures of semiconductors and surrounding environments, such as the solvent and additives.

Influence of Photocatalyst Properties on The Generation and Subsequent Reactions of Radical Intermediates

Semiconductors absorb light with energy larger than their band gaps and produce high-energy carriers to induce LCNA conversion, but semiconductors usually lack suitable active sites to complete the hydrogen evolution reaction. A reduction cocatalyst loaded onto the semiconductor can accumulate photogenerated electrons and catalyze reduction reactions, leaving photogenerated holes on the semiconductor surface to oxidize LCNAs. Studies related to photocatalytic dehydrogenation and dehydrocoupling of LCNAs over semiconductors loaded with reduction cocatalysts are summarized and listed in Table 1:

Table 1. Summary of reaction systems for photocatalytic dehydrogenation and dehydrocoupling of LCNAs over semiconductors loaded with different reduction cocatalysts.

entries	Photocatalysts	Reduction cocatalyst	Substrates	Major oxidized products/Sel. (%)	HER rate (mmol g^{-1} h^{-1})	Reaction conditions	Ref.
1	FP-0.5%Pt/TiO_2	Pt	Methanol	HCHO/98.9	2.81	Pure alcohol	38
2	FP-0.5%Pt/TiO_2	Pt	Methanol	HCHO/65.6	17.38	40% (mole fraction) methanol	38
3	Pt/P25	Pt	Ethanol	Acetal/99.3	79.2[a]	Pure alcohol	39
4	Pt/P25	Pt	1-Propanol	Propylal/99.3	55.3[a]	Pure alcohol	39
5	Pt/P25	Pt	2-Propanol	Acetone/100	11.1[a]	Pure alcohol	39
6	Pd NCs/TiO_2 NS	Pd	Ethanol	Acetal/99.3	51.5	Pure alcohol with 1×10^{-3} mol L^{-1} H^+	40
7	Ni/CdS	Ni	Methanol	HCHO/>99	7.7	Pure alcohol	41
8	Ni/CdS	Ni	Ethanol	Acetaldehyde/>99	10.8	Pure alcohol	41
9	Ni/CdS	Ni	2-Propanol	Acetone/>99	46.6	Pure alcohol	41
10	Ni_2P/CdS	Ni_2P	Methanol	Methylal/77.53	232.77	Pure alcohol with 3×10^{-2} mol L^{-1} H^+	42
11	Ni-MoS_2/CdS	Ni-MoS_2	Ethanol	Acetal/99.2	52.1	Pure alcohol with 3×10^{-2} mol L^{-1} H^+	43
12	CdS-$Ti_3C_2T_x$ MXene	$Ti_3C_2T_x$ MXene	Ethanol	Acetal/85-90	15.4	10 mL of ethanol containing 30 mM H_2SO_4	44
13	CdS + 4 mM $NiCl_2$	Ni	Methanol	HCHO/N/A[b]	48.2	Pure alcohol with 4 mM $NiCl_2$	45
14	AgNPs/CdS	Ag	Ethanol	N/A[b]	1.72	Pure alcohol	46
15	AgNPs/g-C_3N_4	Ag	Methanol	N/A[b]	0.1522	Pure alcohol	47
16	Pt/R-TiO_2	Pt	Ethanol	2,3-BDO/96.6	1.85	30 vol% aqueous solution	48
17	Pt/R-TiO_2	Pt	Ethanol	2,3-BDO/85	N/A[b]	10 vol% aqueous solution	49
18	Pt/F–P25–TiO_2	Pt	Ethanol	2,3-BDO/65	N/A[b]	10 vol% aqueous solution	49
19	MoS_2 foam/CdS	MoS_2	Methanol	EG /91	12	76 wt% CH_3OH+24 wt% H_2O	50
20	Ni_2P/CdS	Ni_2P	Methanol	EG/86.8	0.58	Pure methanol	42
21	CoP/$Zn_2In_2S_5$	CoP	Methanol	EG/90	5.5[a]	76 wt% CH_3OH+24 wt% H_2O	51
22	CoP/$Zn_2In_2S_5$	CoP	Ethanol	2,3-BDO/53	3.2[a]	Pure ethanol	51

23	$NaTaO_3$	None	2-Propanol	Pinacol/74.4	N/A [b]	2.5 M aqueous solution	[52]
24	Gelatinous ZnS	None	Methanol	EG/N/A [b]	1.86	75 vol% aqueous solution	[53]
25	Pt/GO_{NaOH}	Pt	2-Propanol	Pinacol/62.3	6.13	5 vol% aqueous solution	[54]
26	None	None	Ethanol	2,3-BDO/91.3	None	4.8 M aqueous solution and H_2O_2 0.1 mol	[55]

[a] Values calculated are based on the converted alcohols or oxidized products; [b] Means not available. FP: flame pyrolysis; NCs: nanocubes; NS: nanosheets; F–P25: F-modified P25; EG: ethylene glycol; 2,3-BDO: 2,3-butanediol; GO: graphene oxide.

TiO_2 (entries 1-6, 16-18) and CdS (entries 7-14, 19-20) are representative semiconductors that are ultraviolet and visible light responsive, respectively. Metals (entries 1-9, 13-18, 25), metal sulfides (entries 11, 19), metal phosphides (entries 10, 20-22) and MXene (entry 12) are used as reduction cocatalysts, some reactions can also be conducted over semiconductors without cocatalysts (entries 23-24). Except activation by photogenerated carriers, LCNAs can also react with radicals generated by light without the participation of catalysts (entry 26). Generally, the dominant products are carbonyl compounds (entries 1-9, 13-15) for reactions over metal oxides or semiconductors loaded with metallic cocatalysts, while for semiconductors loaded with metal sulfides or phosphides, or without cocatalyst, vicinal diols are the main products (entries 19-24). In addition to the effects of semiconductors and cocatalysts on product selectivity, the solution is also a critical factor that influences the selectivity of products in photocatalytic conversion of LCNAs. Dehydrocoupling reactions are usually reported to be carried out in aqueous solutions (entries 16-19, 21, 23-26) while dehydrogenation in pure alcohols (entries 1, 3-5, 7-9, 13-15) or acidic solution (entries 6, 10-12). In the following sections, the effects of photocatalysts and

reaction environments on product selectivity are discussed. Furthermore, the hydrogen evolution reaction (HER) is also covered. The rate of the dehydrocoupling reaction is generally slower than that of the dehydrogenation reaction, and the reasons are also analyzed in the Summaries and Outlooks.

Selective generation of radical intermediates tuned by the polarity of photocatalyst surfaces

The high selective photocatalytic dehydrogenation of LCNAs over metal oxides can be partially attributed to surface polarity. The polarity of the photocatalyst surface affects the activation priority of C_{α}−H and O−H bonds of LCNAs. A photocatalyst with a polar surface, e.g., TiO_2, catalyzes the O−H bond cleavage in a heterolytic manner. The intrinsic surface polarity of TiO_2 is derived from the large electronegativity difference of Ti (1.54) and O (3.44).[56] In the first step (Figure 4), the LCNA adsorbs onto TiO_2 through −OH, and heterolytically dissociates into an alkoxide and a proton, adsorbing to unsaturated surface Ti^{3+} and O^{2-}, respectively.[57-58] After excitation by light irradiation, photogenerated holes of TiO_2 transfer to surface active sites and oxidize the adsorbed alkoxide followed by the generation of an adsorbed carbon-terminated or oxygen-terminated radical.[59] Subsequently, the adsorbed radical is further oxidized to a carbonyl compound by another photogenerated hole. This step can even conveniently occur spontaneously.[60] The details will be discussed in the following section. In the above process of LCNA conversion, the polar surface of the photocatalysts results in the initial activation of the O−H bond and the generation of adsorbed radical species. These radical intermediates readily undergo further oxidation, rather than C−C bond coupling, because of the restricted diffusion caused by adsorption as well as the

thermodynamic tendency to form carbonyl compounds.

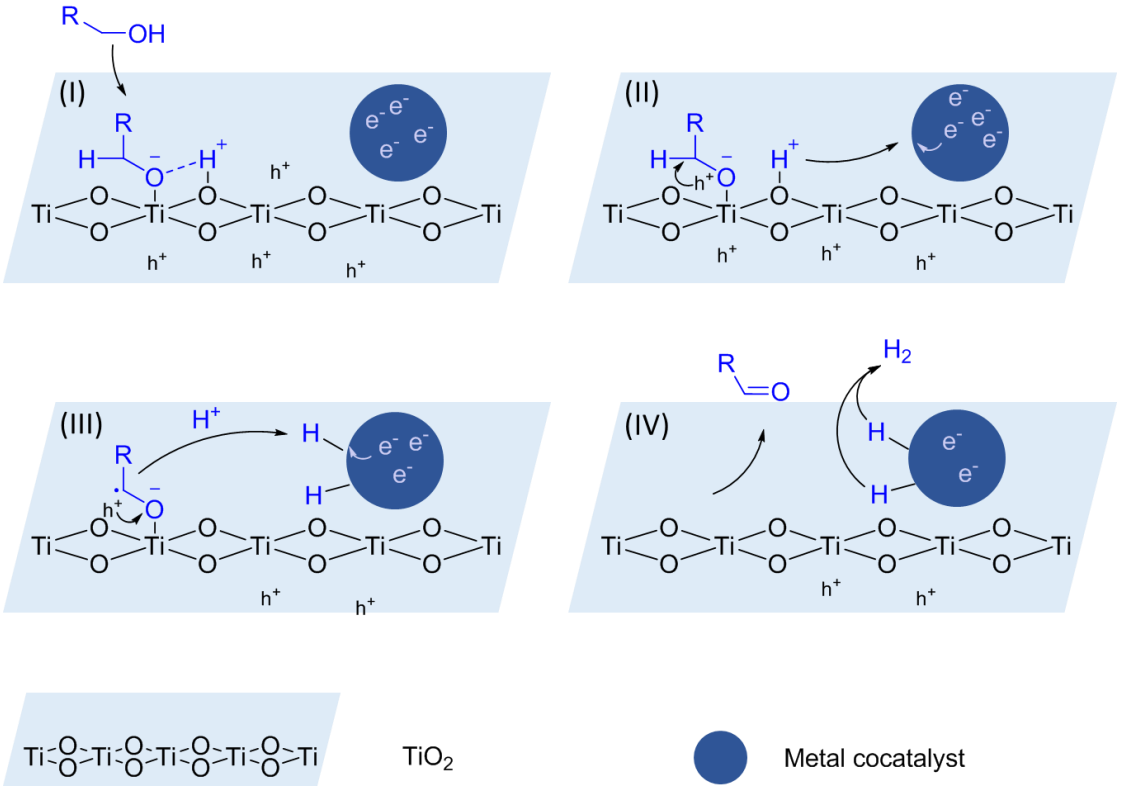

Figure 4. Reaction mechanism of photocatalytic dehydrogenation of LCNAs over metal loaded TiO_2.

Generally, metal sulfides have lower surface polarity. For example, the electronegativity difference of Cd (1.69) and S (2.58) is smaller than that of Ti (1.54) and O (3.44), and smaller than that of H (2.18) and O (3.54).[56] The weak adsorption of −OH on a lower polarity surface, such as metal sulfides, makes the dissociation of −OH more challenging. In this case, the chemical bond is cleaved in a homolytic manner and relies on the BDE of the chemical bond. The BDE of C_α–H bond (< 400 kJ mol^{-1}) is lower than that of the neighboring O–H bond (> 430 kJ mol^{-1}), thus, direct activation of the C_α–H bond to generate a 1-hydroxyalkyl radical is more likely to occur and is thermodynamically favorable. For instance, in 1984, Yanagida *et al.* reported the photocatalytic

dehydrocoupling of methanol to ethylene glycol (EG) over colloidal ZnS.[53] The selectivity of EG was about 75% after 60 h. Due to the wide band gap of ZnS (~3.6 eV), the reaction was irradiated under a high-pressure Hg arc lamp that emits intense visible light. Compared to ZnS, CdS-based photocatalysts are effectively excited by visible light.[61] Thus, they are more commonly used for photocatalysis.[62-64] In other work, Xie and coworkers found that EG was obtained with 90% selectivity over CdS nanorods modified by MoS_2 nanofoams.[50] According to the radical trapping experiments using DMPO (5,5-dimethyl-1-pyrroline N-oxide), the whole process was suggested to be conducted *via* a proton-coupled electron transfer mechanism to form •CH_2OH radicals. Parallel to this work, Chao *et al.* reported 85% selectivity of EG in neat methanol over a Ni_2P/CdS catalyst.[42] Besides CdS, $Zn_2In_2S_5$ was also used to catalyze the production of vicinal diols from LCNAs.[51] The change of product selectivity caused by the different polarity of the catalyst surface was also reported over a GaN photocatalyst.[65-67] The above studies indicate that a weaker polarity surface of the photocatalysts favors their interaction with the alkyl groups of LCNAs, resulting in the preferential activation of the C−H bond. Therefore, if vicinal diols are the target product, semiconductors with low surface polarity would be preferred to improve the product selectivity.

Reactions of radical intermediates affected by the morphology and sizes of photocatalysts

The generated 1-hydroxyalkyl radical intermediates can be further oxidized to carbonyl compounds or undergo C−C bond coupling. Decreasing surface polarity can weaken the adsorption of alcohols, and change the priority for the activation of C_α−H bond and O−H bond. However, unlike alcohols that tend to desorb from catalyst surfaces, 1-hydroxyalkyl radicals are highly

reactive and incline to interact with their surrounding environment, *e.g.*, the catalyst, and be further oxidized. Thus, to obtain vicinal diols, the radical intermediates should be avoided in a confined space where diffusion is limited.

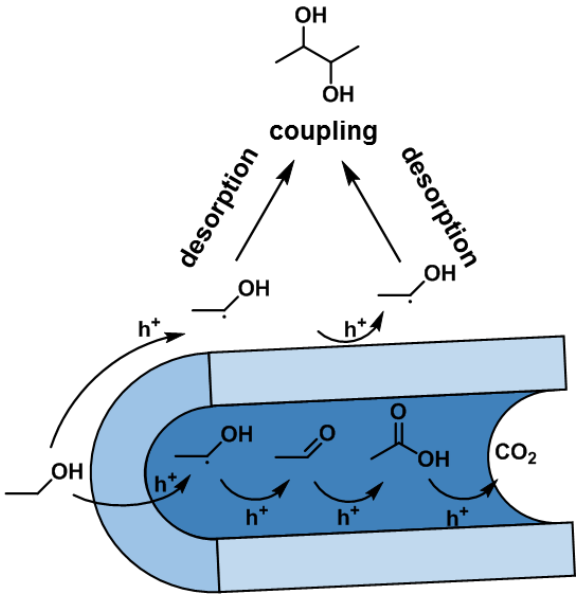

Figure 5. Schematic illustration of varied diffusion of 1-hydroxyethyl radical intermediate on the external surface and the internal channel of TiO_2 nanotubes. Adapted with permission from ref 48. Copyright 2011 Royal Society of Chemistry.

In the dehydrocoupling of LCNAs through the 1-hydroxyalkyl radical, rutile phase TiO_2 with morphology of nanotubes (R-TNTs) and a non-porous structure were compared.[48] The selectivity of 2,3-BDO was 53% over the R-TNTs, while it was more than 90% over the non-porous rutile TiO_2.[48] Considering the possible effects of the pores, liquid paraffin was added to selectively fill the internal space of the R-TNTs to avoid further oxidation of the 1-hydroxyethyl radical on the internal surface (Figure 5), and the selectivity of 2,3-BDO increased from 53% to 86%.[48] These results indicate materials with porous structures having abundant catalytic sites and large specific

surface areas,[68-69] and beneficial for the dehydrogenation reaction, but detrimental for dehydrocoupling of LCNAs due to the adverse effect of radical diffusion in the cavity. For the generated 1-hydroxyalkyl radicals, diffusion into the bulk solution or being further oxidized to carbonyl compounds over the catalyst surface is competitive. If further oxidation to carbonyl compounds is slow, the radicals will have sufficient time to diffuse into the bulk solution and undergo C−C bond coupling.

Table. 2 Comparison of reaction parameters for illuminated 3 nm-ZnS and 4 μm-ZnS particles[70].

Reaction parameter	Particle diameter	
	3 nm-ZnS	4 μm-ZnS
Time interval between two absorption incidences within one particle, $\Delta t = g_{\text{particle}}^{-1}$ (ms)	56.0	19.0×10^{-9}
Time interval between two successive hole transfer processes within one particle, $\Delta t_{\text{transfer}}$ (ms)	306.0	55.0×10^{-6}
Average lifetime of the 1-hydroxyethyl radicals formed (ms)	27.0	-

Further oxidation of adsorbed radical intermediates needs the participation of photogenerated holes, one way to inhibit further oxidation is to extend the time interval between two successive photogenerated holes transferring to surface reaction sites, *i.e.*, reducing the coverage of photogenerated holes on the semiconductor surface. Acetaldehyde and 2,3-BDO were found to be the dominant products over ZnS with sizes of 4 μm and 3 nm, respectively, in photocatalytic ethanol conversion. Based on the experimental physical properties of the two kinds of ZnS (Table 2),[70-71] the time interval between two successive photon absorptions within one particle and two

successive hole transfers to the reaction sites were calculated. These two values for 4 μm-ZnS were nine and seven orders of magnitude smaller than those for 3 nm-ZnS, respectively, indicating faster oxidation of the 1-hydroxyethyl radical to generate acetaldehyde than C−C bond coupling over 4 μm-ZnS. The average lifetime of the 1-hydroxyethyl radical intermediates formed over 3 nm-ZnS was 27 ms, which was shorter than the time interval between two successive hole transfers to the reaction site within one particle (306 ms). Thus, the 1-hydroxyethyl radical had sufficient time to diffuse into the solvent and undergo C−C bond coupling before the next hole transfer when 3 nm-ZnS was used. This result shows that altering the coverage of photogenerated holes transferring to the surface by tuning the particle size of the photocatalyst changes the subsequent transformation paths of adsorbed radical intermediates.

Charge transfer from radical intermediates or substrates to photocatalysts tuned by surface defects

The presence of surface defects can introduce new surface energy levels and provides sites for substrate adsorption, which affects charge transfer between surface adsorbed substrates/intermediates and the photocatalyst. Except for tuning the surface concentration of photogenerated holes to control the selectivity of C−C bond coupling and further dehydrogenation of radical intermediates, surface defects can also affect the selectivity of the two competitive reaction paths. Apart from being oxidized by photogenerated holes, a 1-hydroxyethyl radical can also be oxidized by spontaneously injecting an electron to the conduction band (CB), if the CB position is lower than the oxidation potential of the radical/acetaldehyde.[71-72] In comparison, when

the CB position is high, the electron transfer from the radical or acetaldehyde to ZnS is inhibited (Figure 6a). However, it is difficult to totally remove surface defects during the preparation of ZnS, thus leaving surface defects with energy below the CB of ZnS that can accept electrons. For instance, when 2.6 nm ZnS colloids with 4 mol% excess of Zn^{2+} were used for photocatalytic conversion of ethanol in an inert atmosphere, acetaldehyde rather than 2,3-BDO was the main product. The ZnS colloids exhibited fluorescence at 430 nm, which could be quenched by SH^- ions, indicating the presence of surface sulfur vacancies that located between the CB potential of ZnS and the oxidation potential of the 1-hydroxyl radical and acetaldehyde. During photocatalytic ethanol conversion, sulfur vacancies were suggested to accept electrons from the 1-hydroxyethyl radical which was converted to acetaldehyde (Figure 6b).[71] Similarly, for the reaction over semiconductors with CB positioned lower than the oxidation potential of the radical/acetaldehyde, electron transfer from the radical to the CB is also likely to occur (Figure 6c), the so-called *current doubling reaction.*[60] In summary, trapping energy levels formed by surface defects can change the selectivity of C−C bond coupling and further dehydrogenation *via* controlling the electron transfer channel between photocatalysts and radical intermediates.

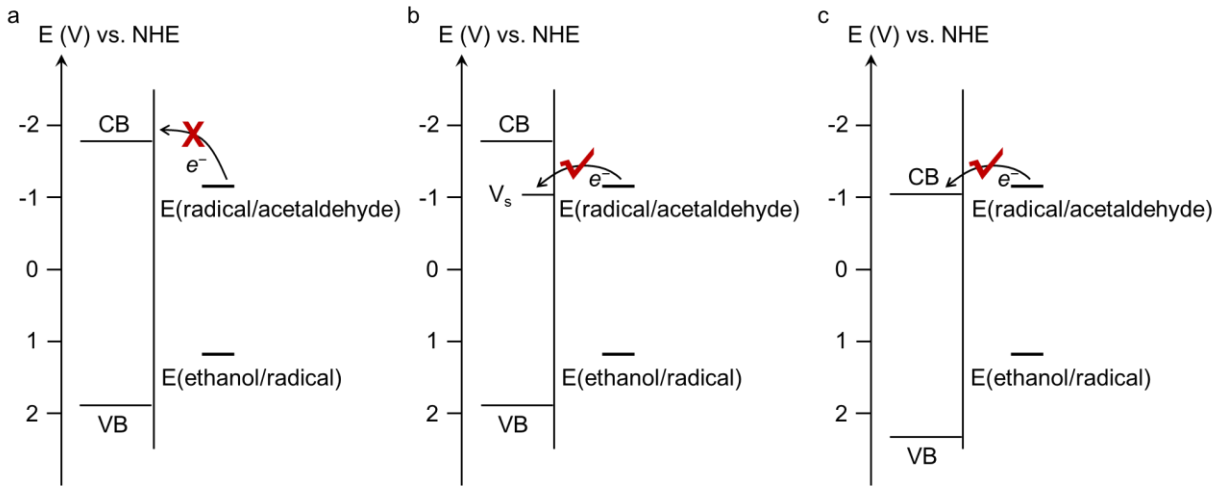

Figure 6. Schematic illustration of electron transfer between photocatalyst and radical controlled by surface defects. **a** and **b**, CB level is located above the redox potential of the radical/acetaldehyde in the absence **(a)** and presence **(b)** of trapping energy levels, respectively. **c**, CB level is located below the oxidation potential of the radical/acetaldehyde. Adapted with permission from ref 71. Copyright 1997 American Chemical Society.

Substrate adsorption is an important step in catalytic reactions, and surface defects can serve as sites for substrate adsorption and activation.[73] By providing adsorption sites, surface defects can affect the activation mode of the substrate, thereby affecting the charge transfer from substrates to catalysts. In the transfer hydrogenation of furfural by using methanol as the hydrogen donor, TiO_2 with morphologies of anatase bipyramids, anatase sheets, and rutile rods were compared, together with the concentrations of surface oxygen vacancies (O_V).[74] Furfural alcohol generated *via* transfer hydrogenation was the dominant product over O_V-rich TiO_2. By contrast, hydrofuroin and furoin from reductive coupling were obtained with a combined selectivity of nearly 100% over O_V-free TiO_2. Density Function Theory (DFT) calculation showed that furfural weakly interacts with O_V-

free TiO_2 with no obvious charge transfer. The oxygen atom of the carbonyl group was negatively charged due to the larger electronegativity of oxygen than that of carbon. In the case of O_V-rich TiO_2, the oxygen atom of the carbonyl group adsorbed to O_V and accepted electrons from nearby Ti^{3+}, thus, a charge redistribution between oxygen and carbon of the carbonyl group might induce negative charges around the carbon atom. The subsequent hydrogen transfer relies considerably on the electron density of the atom of the adsorbed carbonyl group. The atoms of the carbonyl group with a larger electron density is inclined to be hydrogenated and forms carbon- or oxygen-centered radicals (Figure 7). The carbon-centered radicals readily desorb from the surface and couple with each other, while the oxygen-based radicals continue to adsorb on the TiO_2 surface, thus being further hydrogenated. This work shows the mechanism that surface defects affect the electron transfer between the substrate and photocatalyst.

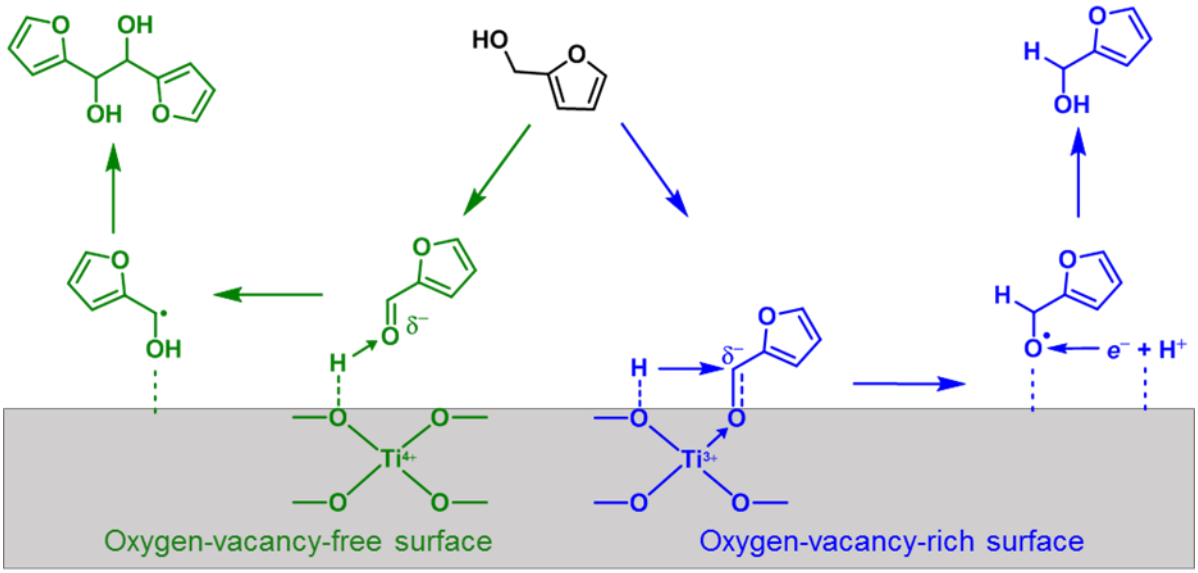

Figure 7. Reaction pathways for the hydrogenation of an aldehyde group and reductive C−C bond coupling over O_V-rich and O_V-free TiO_2, respectively. Reproduced with permission from ref 74. Copyright 2020 Elsevier.

Generation and subsequent reactions of radical intermediates controlled by cocatalysts

Immobilization of reduction cocatalysts onto a photocatalyst can modify the catalyst by introducing active sites, assisting charge transfer and enhancing reactant adsorption.[75-76] Accordingly, cocatalysts are also able to influence the generation and subsequent reactions by several effects, such as the above discussed adsorption and activation of substrates, surface charge carrier coverage and transfer, and surface polarity.

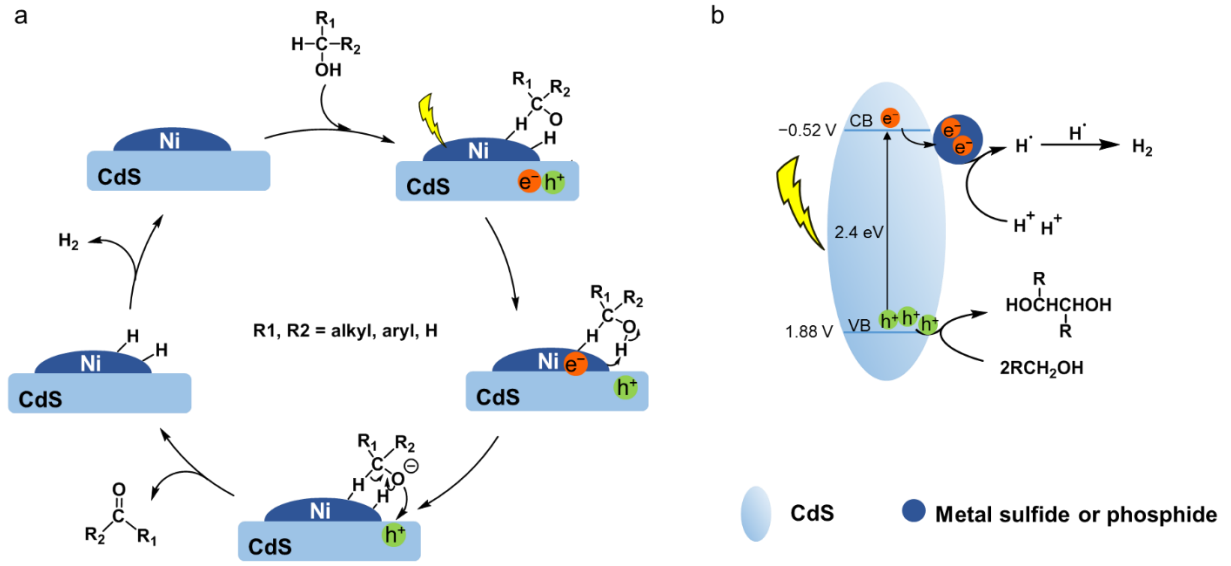

Figure 8. The mechanism of photocatalytic dehydrogenation of LCNAs. a, Over Ni/CdS. Adapted with permission from ref 41. Copyright 2016 American Chemical Society; b, Over MoS_2/CdS.

Metallic reduction cocatalysts can provide adsorption sites for LCNAs and affect the generation of radical intermediates. Higher selectivity of carbonyl compounds is commonly obtained in the presence of metallic reduction cocatalysts. A typical example is the photocatalytic dehydrogenation of LCNAs over a Ni/CdS catalyst.[41] In the reaction system, metallic Ni nanoparticles (NPs) with sizes of 5 nm were deposited onto CdS by *in situ* photo-deposition in

pure alcohols. The Ni/CdS photocatalysts were found to afford quantum yields of 38%, 46% and 48% for methanol, ethanol and isopropanol dehydrogenation, respectively. Another result worth noting is that when benzyl alcohol was used as a substrate, the selectivity shifted towards C−C bond coupling over bare CdS when Ni NPs were absent, indicating the strong effect of metallic Ni on the selectivity of photocatalytic dehydrogenation and dehydrocoupling. These results can be rationally explained by the preferential adsorption of LCNAs at the interface of Ni NPs and CdS. LCNA initially adsorbed on Ni NPs through the O−H bond and was subsequently reduced by photogenerated electrons migrating from CdS to Ni NPs, forming an adsorbed alkoxy anion. Accompanied by the oxidation of the alkoxy anion by photogenerated holes of CdS, the adjacent C_α−H bond was oxidatively cleaved simultaneously (Figure 8a). This mechanism is also supported by aromatic alcohol oxidation to an aromatic aldehyde over nickel-modified metal sulfide photocatalysts.[77-78]

When metal sulfides or phosphides, rather than metallic nanoparticles, are used as reduction cocatalysts, LCNA undergoes C_α−H bond oxidation firstly to generate a 1-hydroxyalkyl radical over the CdS surface. In the subsequent step, the radical intermediates tend to desorb from the CdS surface and couple with each other (Figure 8b).[42, 50] Based on the above-reported mechanism, it seems that metal sulfides cannot activate the O−H bond of LCNAs. By contrast, metal cocatalysts enable the cleavage of the O−H bond as reported in thermocatalytic dehydrogenation of alcohols.[79-80]

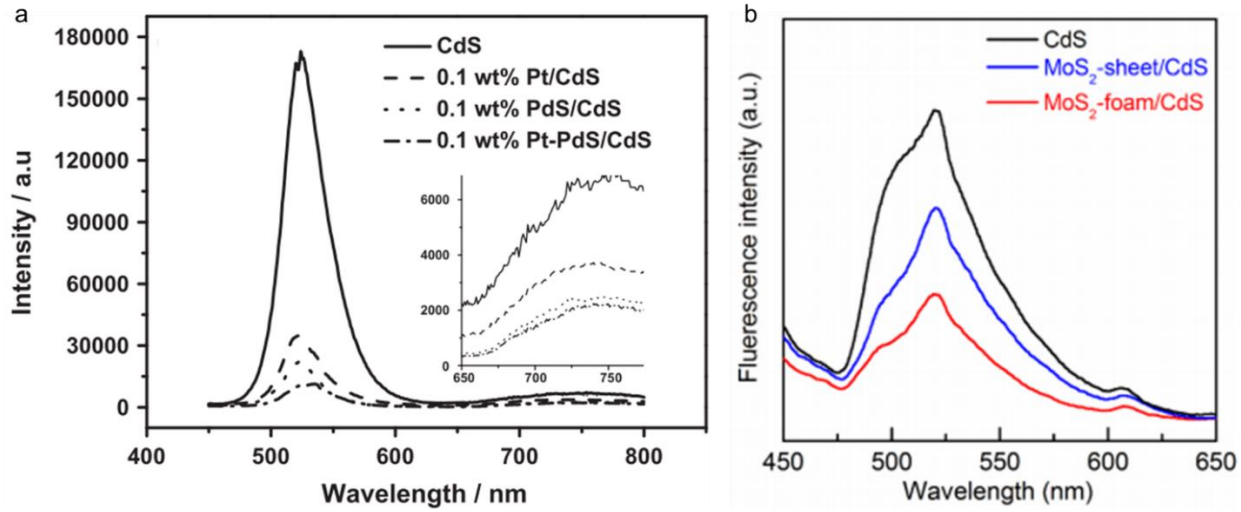

Figure 9. Steady-state photoluminescence emission spectra. **a**, CdS loaded with 0.1 wt% of Pt as reduction cocatalyst. Reprinted with permission from ref 83. Copyright 2012 Elsevier; **b**, CdS loaded with 5 wt% of MoS_2 as reduction cocatalyst. Reprinted with permission from ref 50. Copyright 2018 Springer Nature.

The above-mentioned experimental results of photocatalytic LCNA conversion over ZnS with different particle sizes have proved that increasing the hole coverage is beneficial for the dehydrogenation of LCNA. By contrast, decreasing hole coverage allows radical intermediates to couple with each other. One function of reduction cocatalysts is to accelerate charge separation. The different ability of cocatalysts to aggregate carriers affects surface hole coverage. CdS-based photocatalysts are used as examples to illustrate the effect of loaded cocatalysts on product selectivity of photocatalytic LCNA conversion by altering surface hole coverage. The photogenerated charge carriers over CdS easily recombine,[81] thus, metal or metal sulfide has to be loaded on CdS to increase charge separation. The promotion of charge separation by the cocatalyst can be characterized by measuring the steady-state photoluminescence emission spectrum and

referring to the emission at 530 nm, which can be attributed to the excited electron in CdS relaxing to the ground state.[82] Figure 9 shows the steady-state photoluminescence emission spectra of CdS loaded with 0.1 wt% of Pt (Figure 9a),[83] and 5 wt% of MoS_2 (Figure 9b)[50] as reduction cocatalysts, respectively. 0.1 wt% Pt loaded on CdS can dramatically decrease fluorescence intensity, while the decrease of fluorescence caused by 5 wt% MoS_2 was less evident than that of 0.1 wt% Pt. Although the two catalysts have differences in preparation methods and test conditions, the comparative result of the PL spectra indicates their obviously different abilities to inhibit electron-hole recombination. When metal cocatalysts with a strong ability to promote electron-hole separation are loaded onto semiconductors, surface hole coverage is high, and LCNAs are readily oxidized to carbonyl compounds by two successive photogenerated holes that transfer to the active site. On the contrary, metal sulfide cocatalysts with a relatively weak inhibition ability result in a lower coverage of surface holes and allow radical intermediates to have sufficient time to diffuse into the bulk solution. Bare CdS has the lowest hole coverage, but the selectivity of EG over bare CdS (86.8%) is slightly lower than that over MoS_2/CdS (90%).[42, 50] The reason is that the hole coverage on a bare CdS surface is too low to ensure a critical concentration of radical intermediates in the reaction solution. The C−C bond coupling reaction is a bimolecular reaction, while dehydrogenation is a monomolecular reaction, a high concentration of radical intermediates in the solution will selectively favor the dehydrocoupling reaction.

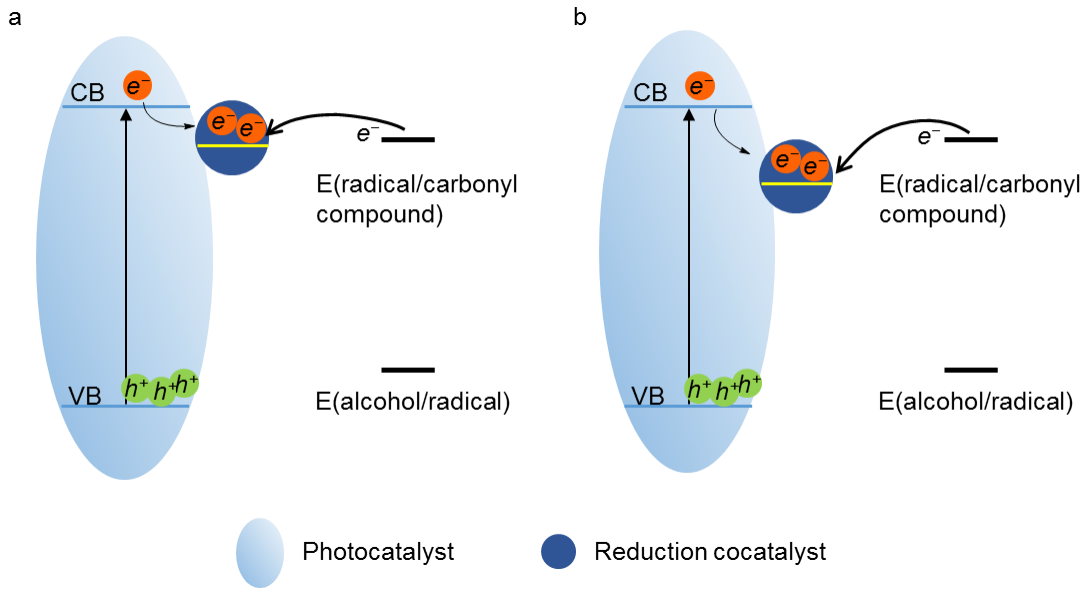

Figure 10. Possible effect of semiconductor surface energy levels introduced by loading nonmetallic (a) or metallic (b) reduction cocatalysts on electron transfer from absorbed radical intermediates to photocatalysts.

Reduction cocatalysts as electron accumulation centers may affect electron transfer processes between radical intermediates and photocatalysts. Noble metals that have relatively large work functions are the most commonly used reduction cocatalysts.[76] The work function of Pt (111) is −5.98 eV.[84] This energy is lower than the CB levels of most metal sulfides.[85] Thus, the energy difference between the redox potential of a radical/carbonyl compound and the Fermi level of the metal cocatalyst is larger than that between this redox potential and the metal sulfide CB energy level. The larger energy difference makes the electron transfer from the adsorbed radical intermediate to the photocatalyst thermodynamically more favorable (Figure 10a, b). Therefore, reduction cocatalysts may affect the surface electronic structure of photocatalysts in a similar way to the effect of surface defects, and changes the conversion pathway of surface radical

intermediates.

The surface polarity of semiconductor photocatalysts may be affected by the preparation process of loading a cocatalyst. The polarity of a semiconductor photocatalyst surface is affected by the electronegativity of surface atoms and the polarity of surface groups. Calcination, hydrothermal, deposition-precipitation and other preparation methods can introduce or remove polar or nonpolar surface moieties and alter adsorption of substrates or radical intermediates, finally influencing product selectivity. In summary, the effects of cocatalyst on product selectivity may also be present in other photocatalytic reactions. Providing more evidence for these factors mentioned above will help to reveal the mechanism of photocatalytic reactions in detail, and is beneficial for developing more effective photocatalysts.

Generation and Subsequent Transformation of Radical Intermediates in The Presence of Water

Production of LCNAs by processes such as CO_2 reduction, CH_4 oxidation, and fermentation is accompanied by the generation of water. Ethanol, propanol, and isopropanol all form azeotropes with water, removing trace amounts of water from LCNAs requires huge energy consumption. Thus, in photocatalytic LCNA conversion, aqueous alcohols are generally used as substrates. In comparison of reactions with pure alcohol, the presence of water changes the rate of conversion and the selectivity of products from photocatalytic conversion of LCNAs in many cases. This is because water in the reaction system may change the activation path of LCNAs or polarity of the

solution.

Generation of radical intermediates initiated by •OH in the presence of water

Early in the 1980s,[86] LCNAs were used as alternatives to water to consume photogenerated holes in photocatalytic water splitting reactions due to the relatively low voltage and overpotential of oxidation. If alcohols are over-oxidized to CO_2, the process is known as photocatalytic reforming of alcohols.[38, 87] TiO_2 loaded with a metal (M/TiO_2) is the most widely used photocatalyst.[88-90] In the presence of water, abundant active species, such as nonselective •OH species,[91] are usually generated. These oxidative species are expected to induce over-oxidation of LCNAs or intermediates to carboxylic acids or CO_2. The non-selective conversion of LCNAs were not discussed here but the intermediates, particularly the •OH radical is of interest here.

The presence of water provides the possibility to generate •OH. An appropriate amount of •OH can control product selectivity by changing the reaction pathway of LCNAs. For example, according to the above sections, when metal oxides with polar surfaces are used as photocatalysts, such as M/TiO_2, the main products are carbonyl compounds. However, vicinal diols can be obtained with more than 65% selectivity over Pt/TiO_2 in aqueous alcohols.[49] This is because in the presence of water, −OH preferentially adsorbs onto the TiO_2 surface,[92, 93] occupying adsorption sites and being oxidized to •OH by photogenerated holes. The produced •OH can directly activate chemical bonds of alcohols, resulting in a reaction mechanism different from that in the absence of water.[49, 94] Besides, if the 1-hydroxyalkyl radical is generated, it is possible to rapidly diffuse into the bulk solution when water is present, so further oxidation of the 1-hydroxyalkyl radical by

surface •OH radical is suppressed. The advantage of inducing a dehydrocoupling reaction by •OH is demonstrated in previous work that used H_2O_2 to produce •OH to trigger the dehydrocoupling of ethanol. The selectivity of 2,3-BDO was reported to reach 91.3%.[55] In addition, water plays an important role in recycling surface −OH of TiO_2,[93] thus, the existence of water is necessary to realize the oxidation of LCNAs through •OH and complete the C−C bond coupling reaction.

Controlling the concentration of •OH is the key to the selective conversion of LCNAs in the presence of water. The dehydrocoupling reactions of LCNAs mainly occur in the solution with a water content of less than 30 vol%, higher water content will cause more production of CO_2 in the photocatalytic aqueous-phase reforming reaction.[38] Hence, controlling the water content is an effective method to avoid over-oxidation caused by excessive •OH.

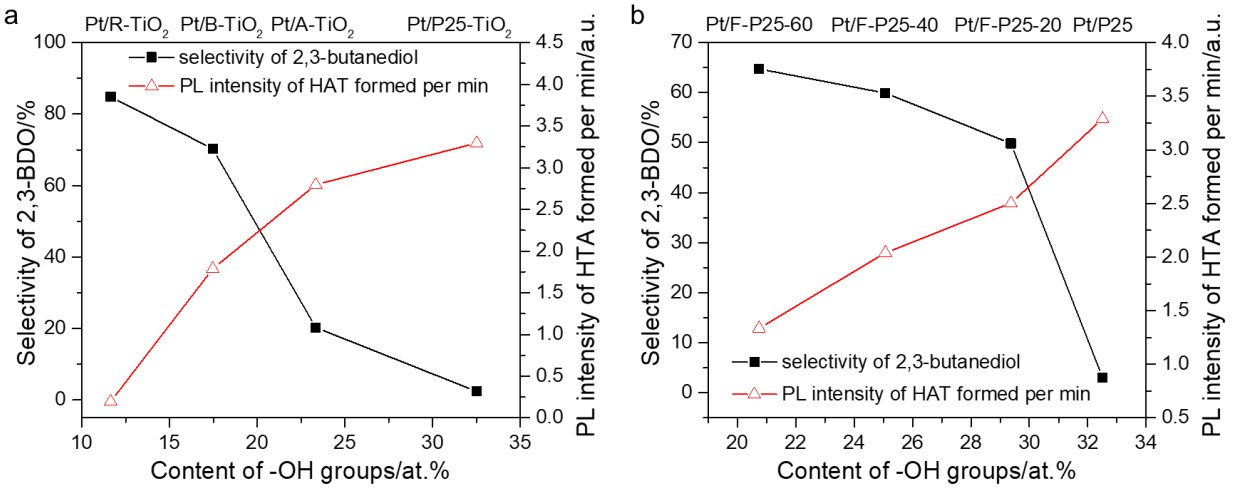

Figure 11. The effect of surface −OH content on the selectivity of 2,3-BDO and PL intensity of HTA formed in the reaction between TA and •OH. a, Pt-decorated Degussa P25-, A-, B-, and R-TiO_2 with different content of surface −OH. A: anatase; B: brookite; R: rutile; P25: Degussa mixed crystal; b, Pt-decorated F-P25-TiO_2 with different amounts of F^- substituted for surface −OH.

Adapted with permission from ref 49. Copyright 2015 Wiley-VCH.

Controlling the content of surface −OH on a TiO_2 surface can tune the •OH concentration. •OH produced in the photocatalytic system can react with terephthalic acid (TA), producing 2-hydroxyterephthalic acid (HTA) of which the photoluminescence emission intensity can be correlated with •OH concentration. Furthermore, XPS (X-ray photoelectron spectroscopy) can be used to quantify surface −OH. These methods provide an accurate way to study the function of surface −OH during photocatalytic conversion of LCNA in the presence of water. By virtue of these methods, Yang and coworkers found a decreased surface −OH content reduced the amount of •OH produced, resulting in 2,3-BDO selectivity increasing from 2.6% to 65% (Figure 11a).[49] The above results were also supported by experiments to control the concentration of surface −OH. Modification by fluoride was used to partially substitute −OH groups on P25-typed TiO_2. When the −OH on the TiO_2 surface decreased, •OH in the solution decreased and the selectivity of 2,3-BDO increased significantly from 2.6% to 85% (Figure 11b). This result further proved that selectivity of photocatalytic dehydrocoupling of LCNA could be efficiently improved by tuning the amount of •OH in the reaction system.

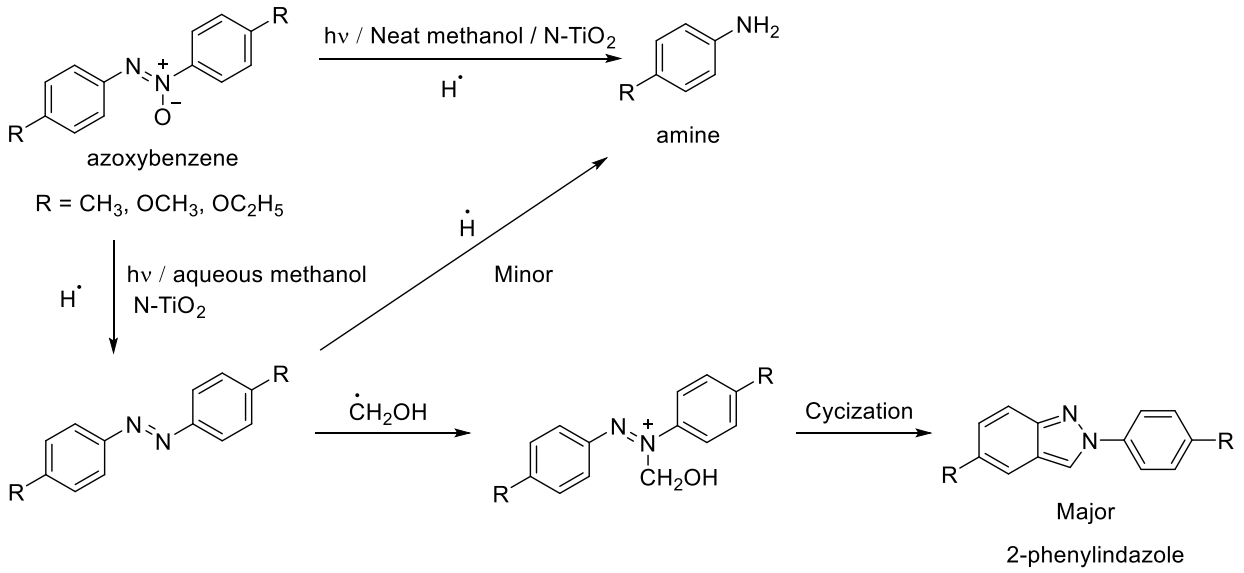

Figure 12. Proposed reaction pathways of methanol and azoxybenzenes in neat methanol and aqueous methanol solution, respectively. Adapted with permission from ref 95. Copyright 2012 Elsevier.

The 1-hydroxyalkyl radical from the oxidation of LCNA by •OH can induce other reactions. Water in the reaction solution was found to change the products of photocatalytic transfer hydrogenation of methanol and azoxybenzene.[95] In an aqueous solution, azoxybenzene reacted with methanol and afforded 2-phenylindazole, by contrast, amine as the hydrogenolysis product of azoxybenzene was obtained in neat methanol (Figure 12). This result was rationalized by the aforementioned role of water in producing •OH. In aqueous methanol a $\bullet CH_2OH$ radical was generated from methanol oxidation by •OH, thus, the $\bullet CH_2OH$ radical easily diffused into the bulk solution and was able to react with the N=N bond. Adversely, methanol was absorbed onto the TiO_2 surface in the absence of water and was directly oxidized by holes, subsequently being oxidized to aldehyde. Therefore, only hydrogen radicals can attack the N=N bond to form complete hydrogenolysis products.

Desorption behavior of radical intermediates in the presence of water

Apart from altering the reaction mechanism *via* the production of •OH and acting as a strong polar protic solvent, water can also increase the polarity of organic solvents. For example, 2% of water in CH_3CN significantly increases the polarity of the mixture from 0.46 for pure CH_3CN (the value for pure water is 1.[96]) to 0.61.[92] In photocatalytic dehydrocoupling of LCNAs, reactive 1-hydroxyalkyl radicals may both interact with the solvent and surface of photocatalysts, and desorption is dependent on the relevant strength of the interaction of the radicals with the solvent and the photocatalyst surface. A solvent with enhanced polarity may have stronger interaction with the −OH of 1-hydroxyalkyl radicals and promote the desorption of the radical from the photocatalyst surface.[49] The effect of water addition in the reaction system is universal, no matter if metal oxide or sulfide semiconductors are used as photocatalysts, thus, the influence of water on radical intermediate desorption is an important phenomenon that needs more comprehensive studies. In conclusion, the presence of water affects the generation of 1-hydroxyalkyl radicals and subsequent reactions in the process of photocatalytic conversion of LCNAs by changing the reaction mechanism and promoting the desorption of the radicals, which is ultimately conducive to the formation of coupling products.

Effect of pH on photocatalytic conversion of LCNAs

An acidic aqueous solution is beneficial for the dehydrogenation reaction of LCNAs, even using a combination of metal sulfide semiconductors and non-metallic reduction cocatalysts, which are preferred for C−C bond coupling reactions. H^+ in solution is from the ionization of the alcohol or

water molecules, or oxidative half-reaction of alcohols, and it has a low concentration. On the contrary, the concentration of H^+ in acidic aqueous solution is high, which is beneficial for the proton transfer and reduction. For example, Chao *et al.* reported that the HER rate was 0.58 mmol g^{-1} h^{-1} over Ni_2P/CdS in pure methanol, and EG was the main product with 86.84% selectivity. When the reaction was carried out in an acidic solution with 3×10^{-2} mol L^{-1} H^+, acetal, from reaction of methanol and formaldehyde, was obtained with 77.53% selectivity. The HER rate was 232.77 mmol g^{-1} h^{-1}, which is 400 times larger than that in pure methanol.[42] The high concentration of H^+ may promote electron consumption, leaving more holes on the catalyst surface. Consequently, the hole concentration on the catalyst surface in acidic aqueous solution may remain at a higher level than in pure alcohol or pure water, which is helpful for the photocatalytic dehydrogenation of LCNAs.

Summaries and Outlooks

Controlling the generation and subsequent transformation of radical intermediates involved in the photocatalytic LCNA conversion is an important way of improving the selectivity of target products. In this context, interactions of alcohols or radical intermediates with the catalyst and the surrounding environment needs to be considered. The interactions, including adsorption, activation, diffusion, and charge transfer, are influenced by the changes in photocatalyst sizes, geometric structures, surface polarities, surface defects, and the nature of reduction cocatalysts. Additionally, surrounding solvents, especially aqueous solutions, affect the activation of LCNAs and the

subsequent reactions of radical intermediates, changing the reaction pathway and influencing product selectivity. Despite these research results, some issues still require further attention.

So far, determining whether a method effectively controls the radical intermediates mainly relies on the evaluation of the reaction activity and selectivity. The characterization methods for free radicals is limited, radical capture experiments can provide information about the types and accumulated concentrations of radicals, *in situ* Electron Paramagnetic Resonance (EPR) spectroscopy shows their instantaneous concentrations. The lack of suitable direct detection methods hinders the direct investigation of the behavior of radical intermediates in real reaction systems. The critical information used to explain the change of radical behavior in different reaction systems, such as lifetime and the interaction between radicals and their surroundings is hard to obtain. Direct measurement of the radical intermediates is a formidable task due to their high reactivity and low abundance in solution. Thus, methodology development for characterization of small molecular radicals during a reaction is helpful, not only for investigating the photocatalytic LCNA conversion, but also for studying other processes that involve small molecular radicals.

The rate of the photocatalytic dehydrocoupling reaction is usually slower than that of the photocatalytic dehydrogenation reaction. Most current methods of improving the dehydrocoupling selectivity slow down the oxidation step of LCNAs, e.g., reducing surface polarity of the photocatalyst weakens the adsorption of alcohols, while adsorption is an effective way for substrate activation; filling the photocatalyst pores by using paraffin reduces the specific surface area of photocatalyst; decreasing the size of the photocatalyst particle and selecting non-noble metal

cocatalyst may cause a lower density of holes. Thus, more effective methods to control the reactivity of small molecular radical intermediates needs to be developed to simultaneously improve the selectivity of target products and the conversion rate of LCNA for practical applications. Furthermore, controlling the reactivity of the radical intermediates from LCNAs is beneficial for the reaction of the radical intermediates and unsaturated compounds or other radicals. Limited studies have focused on this aspect[52, 97-99], and the selectivity needs improvement. This is attributed to the difficulty of controlling small molecular radicals. Hence, more novel reactions are required to be achieved by developing diversified methods of controlling the reactivity of small molecular radicals, and if successful more valuable products would be obtained.

AUTHOR INFORMATION

Corresponding Authors

*N. L.: e-mail, ncluo@dicp.ac.cn.

*F. W.: e-mail, wangfeng@dicp.ac.cn.

ORCID

Zhuyan Gao: 0000-0001-5965-3901

Nengchao Luo: 0000-0002-6137-292X

Zhipeng Huang: 0000-0002-9820-7856

Stuart H. Taylor: 0000-0002-1933-4874

Feng Wang: 0000-0002-9167-8743

Notes

The authors declare no competing financial interest.

Biographies

Zhuyan Gao is currently a PhD candidate in Prof. Feng Wang's group at Dalian Institute of Chemical Physics (DICP), the Chinese Academy of Science. He received his BSc at Huazhong University of Science and Technology in 2016. His research interest focuses on valorization of alcohols by heterogeneous photocatalysis.

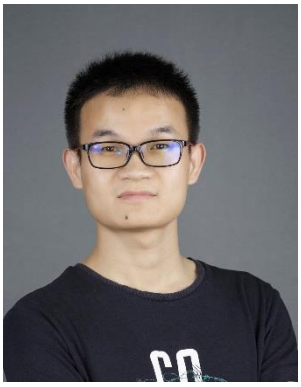

Nengchao Luo received his BSc at Huazhong University of Science and Technology (HUST) in

2014 and PhD at Dalian Institute of Chemical Physics (DICP), Chinese Academy of Sciences in 2020 under the supervision of Prof. Feng Wang. He then joined Prof. Feng Wang's group at DICP, where he was selected as the Excellent Graduate Student of DICP in 2020, and was promoted to an associate professor. His research interests focus on photoreactor design, photocatalysis for biomass upgrading and dehydrocoupling of small molecules.

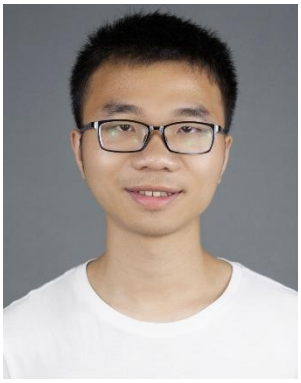

Zhipeng Huang received his BSc from the Huazhong University of Science and Technology (HUST) in 2015. He is currently a PhD candidate in Prof. Feng Wang's group at Dalian Institute of Chemical Physics (DICP), the Chinese Academy of Sciences (CAS). His current research interests include biomass conversion and heterogeneous photoredox catalysis.

Stuart Taylor completed his PhD at the University of Liverpool in 1994, and then took up an academic position at Cardiff University School of Chemistry in 1997. Promoted to Professor in 2013, currently he is the Director of Research for the School and has more than 29 years of experience in heterogeneous catalysis research, publishing over 320 papers and patents. He has wide ranging expertise in experimental studies of catalysis, with his work exploiting preparation techniques for fundamental catalyst understanding and design. His work impacts on chemicals, fuels, sustainability, energy, and the environment. He has many invited presentations at international meetings and has sat on many organizing committees. His research receives support from a wide range of funding bodies and industry. He has collaborated extensively with many universities and industrial groups, both nationally and internationally.

Feng Wang received his BSc at Zhengzhou University (1999) and PhD at Dalian Institute of Chemical Physics (DICP), Chinese Academy of Sciences (2005). He spent 2005–2006 as a postdoctoral fellow at the University of California at Berkeley in USA and 2006–2009 at the Catalysis Research Center of Hokkaido University in Japan. He serves as a full professor and an independent PI at DICP (2009), a joint professor in the State Key Laboratory of Catalysis at DICP (2013), and is the director of the Division of Biomass Conversion & Bio-Energy at DICP (2018 to present). He served as the Cheung Kong Professor at Dalian University of Technology in 2016. His current research focuses on heterogeneous catalysis and biomass conversion.

ACKNOWLEDGMENTS

This work was supported by the National Natural Science Foundation of China (22025206, 21991094, 21721004), the “Strategic Priority Research Program of the Chinese Academy of Sciences” (Grant No. XDB17000000), the “NSFC-RS Newton Advanced Fellowship” of the National Natural Science Foundation of China and Royal Society and the Newton Fund (21961130378, NAF\R1\191267), the Ministry of Science and Technology of the People's

Republic of China (2018YFE0118100), and the CAS - NSTDA Joint Research Project (GJHZ2075).

REFERENCES

1. Kang, J. C.; He, S.; Zhou, W.; Shen, Z.; Li, Y. Y.; Chen, M. S.; Zhang, Q. H.; Wang, Y., Single-pass transformation of syngas into ethanol with high selectivity by triple tandem catalysis. *Nat. Commun.* **2020,** *11*, 827, DOI 10.1038/s41467-020-14672-8.

2. Yang, H.; Zhang, C.; Lai, N.; Huang, B.; Fei, P.; Ding, D.; Hu, P.; Gu, Y.; Wu, H., Efficient isopropanol biosynthesis by engineered Escherichia coli using biologically produced acetate from syngas fermentation. *Bioresour. Technol.* **2020,** *296*, 122337, DOI 10.1016/j.biortech.2019.122337.

3. Chu, W.; Echizen, T.; Kamiya, Y.; Okuhara, T., Gas-phase hydration of ethene over tungstena–zirconia. *Appl. Catal., A* **2004,** *259*, 199-205, DOI 10.1016/j.apcata.2003.09.041.

4. Agarwal, N.; Freakley, S. J.; McVicker, R. U.; Althahban, S. M.; Dimitratos, N.; He, Q.; Morgan, D. J.; Jenkins, R. L.; Willock, D. J.; Taylor, S. H.; Kiely, C. J.; Hutchings, G. J., Aqueous Au-Pd colloids catalyze selective CH_4 oxidation to CH_3OH with O_2 under mild conditions. *Science* **2017,** *358*, 223-227, DOI 10.1126/science.aan6515.

5. Yang, M.; Qi, H.; Liu, F.; Ren, Y.; Pan, X.; Zhang, L.; Liu, X.; Wang, H.; Pang, J.; Zheng, M.; Wang, A.; Zhang, T., One-Pot Production of Cellulosic Ethanol via Tandem Catalysis over a Multifunctional Mo/Pt/WO_x Catalyst. *Joule* **2019,** *3*, 1937-1948, DOI 10.1016/j.joule.2019.05.020.

6. Wang, M.; Liu, M.; Lu, J.; Wang, F., Photo splitting of bio-polyols and sugars to methanol and syngas. *Nat. Commun.* **2020,** *11*, 1083, DOI 10.1038/s41467-020-14915-8.

7. Wang, J.; Tang, C.; Li, G.; Han, Z.; Li, Z.; Liu, H.; Cheng, F.; Li, C., High-Performance M_aZrO_x (Ma = Cd, Ga) Solid-Solution Catalysts for CO_2 Hydrogenation to Methanol. *ACS Catal.* **2019,** *9*, 10253-10259, DOI 10.1021/acscatal.9b03449.

8. Yu, D.; Dai, W.; Wu, G.; Guan, N.; Li, L., Stabilizing copper species using zeolite for ethanol catalytic dehydrogenation to acetaldehyde. *Chin. J. Catal.* **2019,** *40*, 1375-1384, DOI 10.1016/s1872-2067(19)63378-4.

9. Pandey, R. K.; Patnaik, S.; Lakshminarayanan, V., Thin Film of Palladium Nanodendrites Supported on Graphite Electrode for Catalyzing the Oxidation of Small Organic Molecules. *Catal. Lett.* **2014,** *144*, 965-970, DOI 10.1007/s10562-014-1219-3.

10. Leung, A. Y. K.; Hellgardt, K.; Hii, K. K. M., Catalysis in Flow: Nickel-Catalyzed Synthesis of Primary Amines from Alcohols and NH_3. *ACS Sustainable Chem. Eng.* **2018,** *6*, 5479-5484, DOI 10.1021/acssuschemeng.8b00338.

11. Folco, F.; Velasquez Ochoa, J.; Cavani, F.; Ott, L.; Janssen, M., Ethanol gas-phase ammoxidation to acetonitrile: the reactivity of supported vanadium oxide catalysts. *Catal. Sci. Technol.* **2017,** *7*, 200-212, DOI 10.1039/c6cy01275b.

12. Wang, Y.; Furukawa, S.; Yan, N., Identification of an Active NiCu Catalyst for Nitrile Synthesis from Alcohol. *ACS Catal.* **2019,** *9*, 6681-6691, DOI 10.1021/acscatal.9b00043.

13. Rousseau, R.; Dixon, D. A.; Kay, B. D.; Dohnálek, Z., Dehydration, dehydrogenation, and condensation of alcohols on supported oxide catalysts based on cyclic $(WO_3)_3$ and $(MoO_3)_3$ clusters. *Chem. Soc. Rev.* **2014,** *43*, 7664-7680, DOI 10.1039/c3cs60445d.

14. Bravo-Suárez, J. J.; Subramaniam, B.; Chaudhari, R. V., Vapor-phase methanol and ethanol coupling reactions on CuMgAl mixed metal oxides. *Appl. Catal., A* **2013,** *455*, 234-246, DOI 10.1016/j.apcata.2013.01.025.

15. de Souza, E. F.; Pacheco, H. P.; Miyake, N.; Davis, R. J.; Toniolo, F. S., Computational and Experimental Mechanistic Insights into the Ethanol-to-Butanol Upgrading Reaction over MgO. *ACS Catal.* **2020,** *10*, 15162-15177, DOI 10.1021/acscatal.0c04616.

16. Jiang, D.; Fang, G.; Tong, Y.; Wu, X.; Wang, Y.; Hong, D.; Leng, W.; Liang, Z.; Tu, P.; Liu, L.; Xu, K.; Ni, J.; Li, X., Multifunctional Pd@UiO-66 Catalysts for Continuous Catalytic Upgrading of Ethanol to n-Butanol. *ACS Catal.* **2018,** *8*, 11973-11978, DOI 10.1021/acscatal.8b04014.

17. Johnson, T. C.; Morris, D. J.; Wills, M., Hydrogen generation from formic acid and alcohols using homogeneous catalysts. *Chem. Soc. Rev.* **2010,** *39*, 81-88, DOI 10.1039/b904495g.

18. Lin, L.; Zhou, W.; Gao, R.; Yao, S.; Zhang, X.; Xu, W.; Zheng, S.; Jiang, Z.; Yu, Q.; Li, Y. W.; Shi, C.; Wen, X. D.; Ma, D., Low-temperature hydrogen production from water and methanol using Pt/α-MoC catalysts. *Nature* **2017,** *544*, 80-83, DOI 10.1038/nature21672.

19. Nielsen, M.; Alberico, E.; Baumann, W.; Drexler, H. J.; Junge, H.; Gladiali, S.; Beller, M., Low-temperature aqueous-phase methanol dehydrogenation to hydrogen and carbon dioxide. *Nature* **2013,** *495*, 85-89, DOI 10.1038/nature11891.

20. Staffell, I.; Scamman, D.; Velazquez Abad, A.; Balcombe, P.; Dodds, P. E.; Ekins, P.; Shah, N.; Ward, K. R., The role of hydrogen and fuel cells in the global energy system. *Energy Environ. Sci.* **2019,** *12*, 463-491, DOI 10.1039/c8ee01157e.

21. Dawood, F.; Anda, M.; Shafiullah, G. M., Hydrogen production for energy: An overview. *Int. J. Hydrogen Energy* **2020,** *45*, 3847-3869, DOI 10.1016/j.ijhydene.2019.12.059.

22. Luo, Y.-R., *Handbook of Bond Dissociation Energies in Organic Compounds*. 1st ed.; CRC Press LLC: Boca Raton, **2002;** p 392.

23. Matsumura, Y.; Hashimoto, K.; Yoshida, S., Active-Sites for Methanol Dehydrogenation to Formaldehyde on Sodium-Modified Silicalite-1. *J. Catal.* **1991,** *131*, 226-233, DOI 10.1016/0021-9517(91)90339-6.

24. Ren, L.-P.; Dai, W.-L.; Cao, Y.; Li, H.; Fan, K., First observation of highly efficient dehydrogenation of methanol to anhydrous formaldehyde over novel Ag–SiO_2–MgO–Al_2O_3catalyst. *Chem. Commun.* **2003**, 3030-3031, DOI 10.1039/b310316a.

25. Mullen, G. M.; Zhang, L.; Evans, E. J.; Yan, T.; Henkelman, G.; Mullins, C. B., Oxygen and Hydroxyl Species Induce Multiple Reaction Pathways for the Partial Oxidation of Allyl Alcohol on Gold. *J. Am. Chem. Soc.* **2014,** *136*, 6489-6498, DOI 10.1021/ja502347d.

26. Barber, J., Photosynthetic energy conversion: natural and artificial. *Chem. Soc. Rev.* **2009,** *38*, 185-196, DOI 10.1039/b802262n.

27. Lewis, N. S., Toward cost-effective solar energy use. *Science* **2007,** *315*, 798-801, DOI 10.1126/science.1137014.

28. Li, X.; Yu, J. G.; Jaroniec, M.; Chen, X. B., Cocatalysts for Selective Photoreduction of CO_2 into Solar Fuels. *Chem. Rev.* **2019,** *119*, 3962-4179, DOI 10.1021/acs.chemrev.8b00400.

29. Wang, Z.; Li, C.; Domen, K., Recent developments in heterogeneous photocatalysts for solar-driven overall water splitting. *Chem. Soc. Rev.* **2019,** *48*, 2109-2125, DOI 10.1039/c8cs00542g.

30. Yang, X.; Wang, D., Photocatalysis: From Fundamental Principles to Materials and Applications. *ACS Appl. Energy Mater.* **2018,** *1*, 6657-6693, DOI 10.1021/acsaem.8b01345.

31. Yuan, L.; Li, Y.-H.; Tang, Z.-R.; Gong, J.; Xu, Y.-J., Defect-promoted visible light-driven CAC coupling reactions

pairing with CO_2 reduction. *J. Catal.* **2020,** *320*, 244-250, DOI 10.1016/j.jcat.2020.07.036.

32. Xie, S. J.; Ma, W. C.; Wu, X. J.; Zhang, H. K.; Zhang, Q. H.; Wang, Y. D.; Wang, Y., Photocatalytic and electrocatalytic transformations of C1 molecules involving C-C coupling. *Energy Environ. Sci.* **2021,** *14*, 37-89, DOI 10.1039/d0ee01860k.

33. Xia, B.; Zhang, Y.; Shi, B.; Ran, J.; Davey, K.; Qiao, S. Z., Photocatalysts for Hydrogen Evolution Coupled with Production of Value‐Added Chemicals. *Small Methods* **2020,** *4*, 2000063, DOI 10.1002/smtd.202000063.

34. Yang, M. Q.; Xu, Y. J., Selective photoredox using graphene-based composite photocatalysts. *Phys. Chem. Chem. Phys.* **2013,** *15*, 19102-19118, DOI 10.1039/c3cp53325e.

35. Wang, L.; Huang, Z.; Xie, S.; Zhang, Q.; Wang, H.; Wang, Y., Photocatalytic C− H activation and C− C coupling of monohydric alcohols. *Catal. Commun.* **2021,** *153*, 106300, DOI 10.1016/j.catcom.2021.106300.

36. Colmenares, J. C.; Aramendía, M. A.; Marinas, A.; Marinas, J. M.; Urbano, F. J., Synthesis, characterization and photocatalytic activity of different metal-doped titania systems. *Appl. Catal., A* **2006,** *306*, 120-127, DOI 10.1016/j.apcata.2006.03.046.

37. Han, C.; Yang, X.; Gao, G.; Wang, J.; Lu, H.; Liu, J.; Tong, M.; Liang, X., Selective oxidation of methanol to methyl formate on catalysts of Au–Ag alloy nanoparticles supported on titania under UV irradiation. *Green Chem.* **2014,** *16*, 3603-3615, DOI 10.1039/c4gc00367e.

38. Chiarello, G. L.; Aguirre, M. H.; Selli, E., Hydrogen production by photocatalytic steam reforming of methanol on noble metal-modified TiO_2. *J. Catal.* **2010,** *273*, 182-190, DOI 10.1016/j.jcat.2010.05.012.

39. Zhang, H.; Zhu, Z.; Wu, Y.; Zhao, T.; Li, L., TiO_2-photocatalytic acceptorless dehydrogenation coupling of primary alkyl alcohols into acetals. *Green Chem.* **2014,** *16*, 4076-4080, DOI 10.1039/c4gc00413b.

40. Weng, B.; Quan, Q.; Xu, Y.-J., Decorating geometry- and size-controlled sub-20 nm Pd nanocubes onto 2D TiO_2 nanosheets for simultaneous H_2 evolution and 1,1-diethoxyethane production. *J. Mater. Chem. A* **2016,** *4*, 18366-18377, DOI 10.1039/c6ta07853b.

41. Chai, Z.; Zeng, T. T.; Li, Q.; Lu, L. Q.; Xiao, W. J.; Xu, D., Efficient Visible Light-Driven Splitting of Alcohols into Hydrogen and Corresponding Carbonyl Compounds over a Ni-Modified CdS Photocatalyst. *J. Am. Chem. Soc.* **2016,** *138*, 10128-31, DOI 10.1021/jacs.6b06860.

42. Chao, Y.; Lai, J.; Yang, Y.; Zhou, P.; Zhang, Y.; Mu, Z.; Li, S.; Zheng, J.; Zhu, Z.; Tan, Y., Visible light-driven methanol dehydrogenation and conversion into 1,1-dimethoxymethane over a non-noble metal photocatalyst under acidic conditions. *Catal. Sci. Technol.* **2018,** *8*, 3372-3378, DOI 10.1039/c8cy01030g.

43. Chao, Y.; Zhang, W.; Wu, X.; Gong, N.; Bi, Z.; Li, Y.; Zheng, J.; Zhu, Z.; Tan, Y., Visible‐Light Direct Conversion of Ethanol to 1,1‐Diethoxyethane and Hydrogen over a Non‐Precious Metal Photocatalyst. *Chem. Eur. J.* **2018,** *25*, 189-194, DOI 10.1002/chem.201804664.

44. Li, J. Y.; Li, Y. H.; Zhang, F.; Tang, Z. R.; Xu, Y. J., Visible-light-driven integrated organic synthesis and hydrogen evolution over 1D/2D CdS-$Ti_3C_2T_x$ MXene composites. *Appl. Catal., B* **2020,** *269*, 118783, DOI 10.1016/j.apcatb.2020.118783.

45. Huang, H.; Jin, Y.; Chai, Z.; Gu, X.; Liang, Y.; Li, Q.; Liu, H.; Jiang, H.; Xu, D., Surface charge-induced activation of Ni-loaded CdS for efficient and robust photocatalytic dehydrogenation of methanol. *Appl. Catal., B* **2019,** *257*, DOI 10.1016/j.apcatb.2019.117869.

46. Zhang, Q.; Du, C.; Zhao, Q.; Zhou, C.; Yang, S., Visible light-driven the splitting of ethanol into hydrogen and acetaldehyde catalyzed by fibrous AgNPs/CdS hybrids at room temperature. *J. Taiwan Inst. Chem. Eng.* **2019,** *102*, 182-189, DOI 10.1016/j.jtice.2019.05.027.

47. Liu, Y.; Yang, S.; Yin, S.-N.; Feng, L.; Zang, Y.; Xue, H., In situ construction of fibrous AgNPs/g-C_3N_4 aerogel toward light-driven CO_x-free methanol dehydrogenation at room temperature. *Chem. Eng. J.* **2018,** *334*, 2401-2407, DOI 10.1016/j.cej.2017.12.016.

48. Lu, H.; Zhao, J.; Li, L.; Gong, L.; Zheng, J.; Zhang, L.; Wang, Z.; Zhang, J.; Zhu, Z., Selective oxidation of sacrificial ethanol over TiO_2-based photocatalysts during water splitting. *Energy Environ. Sci.* **2011,** *4*, 3384-3388, DOI 10.1039/c1ee01476e.

49. Yang, P.; Zhao, J.; Cao, B.; Li, L.; Wang, Z.; Tian, X.; Jia, S.; Zhu, Z., Selective Photocatalytic C–C Coupling of Bioethanol into 2,3-Butanediol over Pt-Decorated Hydroxyl-Group-Tunable TiO_2 Photocatalysts. *ChemCatChem* **2015,** *7*, 2384-2390, DOI 10.1002/cctc.201500326.

50. Xie, S.; Shen, Z.; Deng, J.; Guo, P.; Zhang, Q.; Zhang, H.; Ma, C.; Jiang, Z.; Cheng, J.; Deng, D.; Wang, Y., Visible light-driven C–H activation and C–C coupling of methanol into ethylene glycol. *Nat. Commun.* **2018,** *9*, 1181, DOI 10.1038/s41467-018-03543-y.

51. Zhang, H.; Xie, S.; Hu, J.; Wu, X.; Zhang, Q.; Cheng, J.; Wang, Y., C–H activations of methanol and ethanol and C–C couplings into diols by zinc–indium–sulfide under visible light. *Chem. Commun.* **2020,** *56*, 1776-1779, DOI 10.1039/c9cc09205f.

52. Cao, B.; Zhang, J.; Zhao, J.; Wang, Z.; Yang, P.; Zhang, H.; Li, L.; Zhu, Z., Cooperative Dehydrogenation Coupling of Isopropanol and Hydrogenation Coupling of Acetone Over a Sodium Tantalate Photocatalyst. *ChemCatChem* **2014,** *6*, 1673-1678, DOI 10.1002/cctc.201400032.

53. Yanagida, S.; Azuma, T.; Kawakami, H.; Kizumoto, H.; Sakurai, H., Photocatalytic Carbon Carbon Bond Formation with Concurrent Hydrogen Evolution on Colloidal Zinc Sulphide. *J. Chem. Soc., Chem. Commun.* **1984**, 21-22, DOI 10.1039/C39840000021.

54. Cao, B.; Yu, Y.; Xu, S.; Qu, J.; Gao, G.; Li, H.; Gao, N.; Ren, Y.; Zhou, C., Selective photocatalytic C–C coupling of isopropanol into pinacol with concurrent hydrogen evolution over GO_{NaOH} photocatalyst. *New J. Chem.* **2019,** *43*, 1936-1942, DOI 10.1039/c8nj02348d.

55. Li, N.; Yan, W.; Yang, P.; Zhang, H.; Wang, Z.; Zheng, J.; Jia, S.; Zhu, Z., Direct C–C coupling of bio-ethanol into 2,3-butanediol by photochemical and photocatalytic oxidation with hydrogen peroxide. *Green Chem.* **2016,** *18*, 6029-6034, DOI 10.1039/c6gc00883f.

56. Allred, A. L., Electronegativity Values from Thermochemical Data. *J. Inorg. Nucl. Chem.* **1961,** *17*, 215-221, DOI 10.1016/0022-1902(61)80142-5.

57. Murdoch, M.; Waterhouse, G. I. N.; Nadeem, M. A.; Metson, J. B.; Keane, M. A.; Howe, R. F.; Llorca, J.; Idriss, H., The effect of gold loading and particle size on photocatalytic hydrogen production from ethanol over Au/TiO_2 nanoparticles. *Nat. Chem.* **2011,** *3*, 489-492, DOI 10.1038/nchem.1048.

58. Guo, Q.; Xu, C.; Ren, Z.; Yang, W.; Ma, Z.; Dai, D.; Fan, H.; Minton, T. K.; Yang, X., Stepwise Photocatalytic Dissociation of Methanol and Water on TiO_2(110). *J. Am. Chem. Soc.* **2012,** *134*, 13366-13373, DOI 10.1021/ja304049x.

59. Zhang, J.; Peng, C.; Wang, H.; Hu, P., Identifying the Role of Photogenerated Holes in Photocatalytic Methanol Dissociation on Rutile TiO_2(110). *ACS Catal.* **2017,** *7*, 2374-2380, DOI 10.1021/acscatal.6b03348.

60. Yamagata, S.; Nakabayashi, S.; Sancier, K. M.; Fujishima, A., Photocatalytic Oxidation of Alcohols on TiO_2. *Bull. Chem. Soc. Jpn.* **1988,** *61*, 3429-3434, DOI 10.1246/bcsj.61.3429.

61. Li, J. Y.; Li, Y. H.; Qi, M. Y.; Lin, Q.; Tang, Z. R.; Xu, Y. J., Selective Organic Transformations over Cadmium Sulfide-Based Photocatalysts. *ACS Catal.* **2020,** *10*, 6262-6280, DOI 10.1021/acscatal.0c01567.

62. Qi, M. Y.; Li, Y. H.; Anpo, M.; Tang, Z. R.; Xu, Y. J., Efficient Photoredox-Mediated C-C Coupling Organic Synthesis and Hydrogen Production over Engineered Semiconductor Quantum Dots. *ACS Catal.* **2020,** *10*, 14327-14335, DOI 10.1021/acscatal.0c04237.

63. Han, C.; Tang, Z.-R.; Liu, J.; Jin, S.; Xu, Y.-J., Efficient photoredox conversion of alcohol to aldehyde and H_2 by heterointerface engineering of bimetal–semiconductor hybrids. *Chem. Sci.* **2019,** *10*, 3514-3522, DOI 10.1039/C8SC05813J.

64. Li, Y.-H.; Zhang, F.; Chen, Y.; Li, J.-Y.; Xu, Y.-J., Photoredox-catalyzed biomass intermediate conversion integrated with H_2 production over $Ti_3C_2T_x$/CdS composites. *Green Chem.* **2020,** *22*, 163-169, DOI 10.1039/c9gc03332g.

65. Liu, M.; Wang, Y.; Kong, X.; Rashid, R. T.; Chu, S.; Li, C.-C.; Hearne, Z.; Guo, H.; Mi, Z.; Li, C.-J., Direct Catalytic Methanol-to-Ethanol Photo-conversion via Methyl Carbene. *Chem* **2019,** *5*, 858-867, DOI 10.1016/j.chempr.2019.01.005.

66. Li, L.; Fan, S. Z.; Mu, X. Y.; Mi, Z. T.; Li, C. J., Photoinduced Conversion of Methane into Benzene over GaN Nanowires. *J. Am. Chem. Soc.* **2014,** *136*, 7793-7796, DOI 10.1021/ja5004119.

67. Li, L.; Mu, X. Y.; Liu, W. B.; Kong, X. H.; Fan, S. Z.; Mi, Z. T.; Li, C. J., Thermal Non-Oxidative Aromatization of Light Alkanes Catalyzed by Gallium Nitride. *Angew. Chem., Int. Ed.* **2014,** *53*, 14106-14109, DOI 10.1002/anie.201408754.

68. Joo, J. B.; Dahl, M.; Li, N.; Zaera, F.; Yin, Y., Tailored synthesis of mesoporous TiO_2 hollow nanostructures for catalytic applications. *Energy Environ. Sci.* **2013,** *6*, 2082-2092, DOI 10.1039/c3ee41155a.

69. Zhang, W.; Tian, Y.; He, H.; Xu, L.; Li, W.; Zhao, D., Recent advances in the synthesis of hierarchically mesoporous TiO_2 materials for energy and environmental applications. *Natl. Sci. Rev.* **2020,** *7*, 1702-1725, DOI 10.1093/nsr/nwaa021.

70. Müller, B. R.; Majoni, S.; Meissner, D.; Memming, R., Photocatalytic oxidation of ethanol on micrometerand nanometer-sized semiconductor particles. *J. Photoch. Photobio., A* **2002,** *151*, 253-265, DOI 10.1016/S1010-6030(02)00010-2.

71. Muller, B. R.; Majoni, S.; Memming, R.; Meissner, D., Particle size and surface chemistry in photoelectrochemical reactions at semiconductor particles. *J. Phys. Chem. B* **1997,** *101*, 2501-2507, DOI 10.1021/jp962749v.

72. Lilie, V. J.; Beck, G.; Henglein, A., Pulsradiolyse und Polarographie : Halbstufenpotentiale fur die Oxydation und Reduktion von kurzlebigen organischen Radikalen an der Hg-Elektrode. *Ber. Bunsen Ges. Phys. Chem.* **1971,** *75*, 458-465, DOI 10.1002/bbpc.19710750513.

73. Li, H.; Shang, J.; Ai, Z.; Zhang, L., Efficient Visible Light Nitrogen Fixation with BiOBr Nanosheets of Oxygen Vacancies on the Exposed {001} Facets. *J. Am. Chem. Soc.* **2015,** *137*, 6393-6399, DOI 10.1021/jacs.5b03105.

74. Wu, X.; Li, J.; Xie, S.; Duan, P.; Zhang, H.; Feng, J.; Zhang, Q.; Cheng, J.; Wang, Y., Selectivity Control in Photocatalytic Valorization of Biomass-Derived Platform Compounds by Surface Engineering of Titanium Oxide. *Chem* **2020,** *6*, 3038-3053, DOI 10.1016/j.chempr.2020.08.014.

75. Meng, A. Y.; Zhang, L. Y.; Cheng, B.; Yu, J. G., Dual Cocatalysts in TiO_2 Photocatalysis. *Adv. Mater.* **2019,** *31*, 1807660, DOI 10.1002/adma.201807660.

76. Yang, J. H.; Wang, D. G.; Han, H. X.; Li, C., Roles of Cocatalysts in Photocatalysis and Photoelectrocatalysis. *Acc. Chem. Res.* **2013,** *46*, 1900-1909, DOI 10.1021/ar300227e.

77. Han, G.; Jin, Y. H.; Burgess, R. A.; Dickenson, N. E.; Cao, X. M.; Sun, Y., Visible-Light-Driven Valorization of

Biomass Intermediates Integrated with H_2 Production Catalyzed by Ultrathin Ni/CdS Nanosheets. *J. Am. Chem. Soc.* **2017,** *139*, 15584-15587, DOI 10.1021/jacs.7b08657.

78. Lin, Q.; Li, Y. H.; Qi, M. Y.; Li, J. Y.; Tang, Z. R.; Anpo, M.; Yamada, Y. M. A.; Xu, Y. J., Photoredox dual reaction for selective alcohol oxidation and hydrogen evolution over nickel surface-modified $ZnIn_2S_4$. *Appl. Catal., B* **2020,** *271*, 118946, DOI 10.1016/j.apcatb.2020.118946.

79. Chen, J.; Zhang, Q.; Fang, W.; Wang, Y.; Wan, H., Oxidant-Free Dehydrogenation of Alcohols over Hydrotalcite-Supported Palladium Catalysts. *Chin. J. Catal.* **2010,** *31*, 1061-1070, DOI 10.3724/sp.J.1088.2010.00505.

80. Kon, K.; Hakim Siddiki, S. M. A.; Shimizu, K.-i., Size- and support-dependent Pt nanocluster catalysis for oxidant-free dehydrogenation of alcohols. *J. Catal.* **2013,** *304*, 63-71, DOI 10.1016/j.jcat.2013.04.003.

81. Cheng, L.; Xiang, Q.; Liao, Y.; Zhang, H., CdS-Based photocatalysts. *Energy Environ. Sci.* **2018,** *11*, 1362-1391, DOI 10.1039/c7ee03640j.

82. Zhai, T.; Fang, X.; Li, L.; Bando, Y.; Golberg, D., One-dimensional CdS nanostructures: synthesis, properties, and applications. *Nanoscale* **2010,** *2*, 168-187, DOI 10.1039/b9nr00415g.

83. Yang, J.; Yan, H.; Wang, X.; Wen, F.; Wang, Z.; Fan, D.; Shi, J.; Li, C., Roles of cocatalysts in Pt–PdS/CdS with exceptionally high quantum efficiency for photocatalytic hydrogen production. *J. Catal.* **2012,** *290*, 151-157, DOI 10.1016/j.jcat.2012.03.008.

84. Derry, G. N.; Ji-Zhong, Z., Work function of Pt(111). *Phys. Rev. B* **1989,** *39*, 1940-1941, DOI 10.1103/PhysRevB.39.1940.

85. Xu, Y.; Schoonen, M. A. A., The absolute energy positions of conduction and valence bands of selected semiconducting minerals. *Am. Mineral.* **2000,** *85*, 543-556, DOI 10.2138/am-2000-0416.

86. Kawai, T.; Sakata, T., Photocatalytic Hydrogen-Production from Liquid Methanol and Water. *J. Chem. Soc., Chem. Commun.* **1980**, 694-695, DOI 10.1039/c39800000694.

87. Tan, H.; Kong, P.; Liu, M.; Gu, X.; Zheng, Z., Enhanced photocatalytic hydrogen production from aqueous-phase methanol reforming over cyano-carboxylic bifunctionally-modified carbon nitride. *Chem. Commun.* **2019,** *55*, 12503-12506, DOI 10.1039/c9cc06600d.

88. Yang, Y.; Chang, C.; Idriss, H., Photo-catalytic production of hydrogen form ethanol over M/TiO_2 catalysts (M=Pd, Pt or Rh). *Appl. Catal., B* **2006,** *67*, 217-222, DOI 10.1016/j.apcatb.2006.05.007.

89. Chen, W.-T.; Chan, A.; Sun-Waterhouse, D.; Moriga, T.; Idriss, H.; Waterhouse, G. I. N., Ni/TiO_2: A promising low-cost photocatalytic system for solar H_2 production from ethanol–water mixtures. *J. Catal.* **2015,** *326*, 43-53, DOI 10.1016/j.jcat.2015.03.008.

90. Nadeem, M. A.; Murdoch, M.; Waterhouse, G. I. N.; Metson, J. B.; Keane, M. A.; Llorca, J.; Idriss, H., Photoreaction of ethanol on Au/TiO_2 anatase: Comparing the micro to nanoparticle size activities of the support for hydrogen production. *J. Photochem. Photobiol., A* **2010,** *216*, 250-255, DOI 10.1016/j.jphotochem.2010.07.007.

91. Shinde, S. S.; Bhosale, C. H.; Rajpure, K. Y., Kinetic Analysis of Heterogeneous Photocatalysis: Role of Hydroxyl Radicals. *Catal. Rev.* **2013,** *55*, 79-133, DOI 10.1080/01614940.2012.734202.

92. Molinari, A.; Montoncello, M.; Rezala, H.; Maldotti, A., Partial oxidation of allylic and primary alcohols with O_2 by photoexcited TiO_2. *Photochem. Photobiol. Sci.* **2009,** *8*, 613-619, DOI 10.1039/b817147e.

93. Zhang, H.; Zhang, W.; Zhao, M.; Yang, P.; Zhu, Z., A site-holding effect of TiO_2 surface hydroxyl in the photocatalytic direct synthesis of 1,1-diethoxyethane from ethanol. *Chem. Commun.* **2017,** *53*, 1518-1521, DOI 10.1039/c6cc09050h.

94. Dvoranová, D.; Barbieriková, Z.; Brezová, V., Radical Intermediates in Photoinduced Reactions on TiO_2 (An

EPR Spin Trapping Study). *Molecules* **2014,** *19*, 17279-17304, DOI 10.3390/molecules191117279.

95. Selvam, K.; Balachandran, S.; Velmurugan, R.; Swaminathan, M., Mesoporous nitrogen doped nano titania—A green photocatalyst for the effective reductive cleavage of azoxybenzenes to amines or 2-phenyl indazoles in methanol. *Appl. Catal., A* **2012,** *413-414*, 213-222, DOI 10.1016/j.apcata.2011.11.011.

96. Reichardt, C., Solvatochromic Dyes as Solvent Polarity Indicators. *Chem. Rev.* **1994,** *94*, 2319-2358, DOI 10.1021/cr00032a005.

97. Griesbeck, A. G.; Reckenthäler, M., Homogeneous and heterogeneous photoredox-catalyzed hydroxymethylation of ketones and keto esters: catalyst screening, chemoselectivity and dilution effects. *Beilstein J. Org. Chem.* **2014,** *10*, 1143-1150, DOI 10.3762/bjoc.10.114.

98. Fan, Y.; Bao, J.; Shi, L.; Li, S.; Lu, Y.; Liu, H.; Wang, H.; Zhong, L.; Sun, Y., Photocatalytic Coupling of Methanol and Formaldehyde into Ethylene Glycol with High Atomic Efficiency. *Catal. Lett.* **2018,** *148*, 2274-2282, DOI 10.1007/s10562-018-2465-6.

99. Bao, J.; Fan, Y.; Zhang, S.; Zhong, L.; Wu, M.; Sun, Y., Hydrofunctionalization of Olefins to Higher Aliphatic Alcohols via Visible-Light Photocatalytic Coupling. *Catal. Lett.* **2019,** *149*, 1651-1659, DOI 10.1007/s10562-019-02737-3.

For Table of Contents Use Only

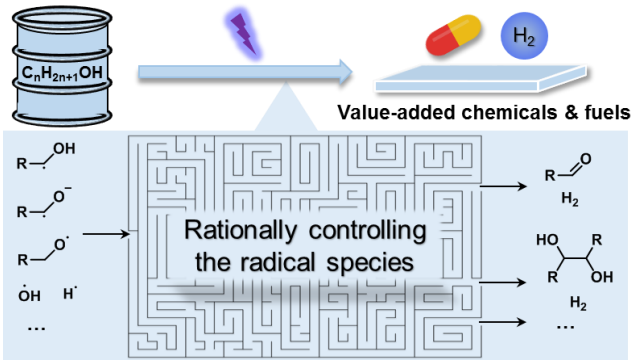

Synopsis: Valued-added chemicals and fuels can be produced from sustainable low-carbon-number alcohols by controlling the radical intermediates in photocatalytic conversion processes.